

The skew T diagram, and atmospheric stability

Table of contents

1. The aerological diagram	4
<i>i. Radiosondes</i>	4
<i>ii. Hydrostatic balance; the hypsometric equation</i>	4
<i>iii. Aerological diagrams</i>	6
2. Skew T applications	10
(i) <i>The skew T diagram</i>	10
(ii) <i>Determination of moisture parameters</i>	11
(iii) <i>Lifting condensation level (LCL)</i>	13
(iv) <i>Potential temperature</i>	13
(v) <i>Moist potential temperatures</i>	17
(vi) <i>Normand’s rule</i>	20
(vii) <i>Convection condensation level (CCL)</i>	21
(viii) <i>Some other applications</i>	22
(a) Thickness (δz)	22
(b) Precipitable water (PW)	25
(c) Föhn effect:	25
(d) Large scale subsidence	26
(e) Turbulent mixing in the PBL	26
(f) Conservative variables	26
3. Static stability	28
(i) <i>The concept of stability</i>	28
(ii) <i>The parcel technique</i>	28
(a) Stable, neutral and unstable	28
(b) Local and non-local stability	31
(c) Absolute and conditional stability	33
(iii) <i>The slope technique</i>	34
(iv) <i>Conditional instability</i>	35
(v) <i>Convective available potential energy (CAPE), and convective inhibition (CIN)</i>	37
(vi) <i>Latent instability</i>	40
(vii) <i>Potential instability</i>	43
(viii) <i>Profiles of θ_e, θ_e^*, and CAPE</i>	46
(ix) <i>Stability indices</i>	47
References	48

List of symbols, units and numerical values

SOME USEFUL NUMERICAL VALUES

Quantity	Name of unit	Symbol	Definition
Basic units			
Length	meter	m	
Mass	kilogram	kg	
Time	second	s	
Electrical current	ampere	A	
Temperature	degree Kelvin	°K	
Derived units			
Force	newton	N	kg m s ⁻²
Pressure	pascal	Pa	N m ⁻² = kg m ⁻¹ s ⁻²
Energy	joule	J	kg m ² s ⁻²
Power	watt	W	J s ⁻¹ = kg m ² s ⁻³
Electrical potential difference	volt	V	W A ⁻¹ = kg m ² s ⁻³ A ⁻¹
Electrical charge	coulomb	C	A s
Electrical resistance	ohm	Ω	V A ⁻¹ = kg m ² s ⁻³ A ⁻²
Electrical capacitance	farad	F	A s V ⁻¹ = kg ⁻¹ m ⁻² s ⁴ A ²
Frequency	hertz	Hz	s ⁻¹
Celsius temperature	degree Celsius	°C	°K – 273.15
Temperature interval	degree	deg or °	K or C need not be specified
Acceptable			
Volume	liter	l	10 ⁻³ m ³
Pressure	millibar	mbar	10 ² Pa
		(abbreviated to mb in this book)	
The following prefixes are used to construct decimal multiples of units.			
<i>Multiple</i>	<i>Prefix</i>	<i>Symbol</i>	<i>Multiple</i> <i>Prefix</i> <i>Symbol</i>
10 ⁻¹	deci	d	10 deca da
10 ⁻²	centi	c	10 ² hecto h
10 ⁻³	milli	m	10 ³ kilo k
10 ⁻⁶	micro	μ	10 ⁶ mega M
10 ⁻⁹	nano	n	10 ⁹ giga G
10 ⁻¹²	pico	p	10 ¹² tera T
10 ⁻¹⁵	femto	f	
10 ⁻¹⁸	atto	a	
Universal constants			
	Universal gas constant (<i>R</i> *)		8.3143 × 10 ³ J deg ⁻¹ kmol ⁻¹
	Boltzmann's constant (<i>k</i>)		1.381 × 10 ⁻²³ J deg ⁻¹ molecule ⁻¹
	Avogadro's number (<i>N_A</i>)		6.022 × 10 ²⁶ kmol ⁻¹
	Stefan-Boltzmann constant (<i>σ</i>)		5.6696 × 10 ⁻⁸ W m ⁻² deg ⁻⁴
	Planck's constant (<i>h</i>)		6.6262 × 10 ⁻³⁴ J s
	Velocity of light (<i>c</i> *)		2.998 × 10 ⁸ m s ⁻¹
	Permittivity of a vacuum (<i>ε₀</i>)		8.85 × 10 ⁻¹² C ² N ⁻¹ m ⁻²
The earth			
	Average radius (<i>R_E</i>)		6.37 × 10 ⁶ m
	Acceleration due to gravity at surface of earth (<i>g₀</i>)		9.81 m s ⁻²
			7.292 × 10 ⁻⁵ rad s ⁻¹
	Angular velocity of rotation (<i>Ω</i>)		
	Average distance from sun to surface of earth (<i>d</i>)		1.50 × 10 ¹¹ m
	Solar irradiance on a perpendicular plane at distance <i>d</i> from sun		1.38 × 10 ³ W m ⁻²
Dry air			
	Apparent molecular weight (<i>M_d</i>)		28.97
	Gas constant (<i>R_d</i>)		287 J deg ⁻¹ kg ⁻¹
	Density at 0°C and 1000 mb pressure (varies as <i>p/T</i>)		1.275 kg m ⁻³
	Specific heat at constant pressure (<i>c_p</i>)		1004 J deg ⁻¹ kg ⁻¹
	Specific heat at constant volume (<i>c_v</i>)		717 J deg ⁻¹ kg ⁻¹
	Thermal conductivity at 0°C (independent of pressure)		2.40 × 10 ⁻² J m ⁻¹ s ⁻¹ deg ⁻¹
Water substance			
	Molecular weight (<i>M_w</i>)		18.016
	Gas constant for water vapor (<i>R_v</i>)		461 J deg ⁻¹ kg ⁻¹
	Density of liquid water at 0°C		1.000 × 10 ³ kg m ⁻³
	Density of ice at 0°C		0.917 × 10 ³ kg m ⁻³
	Specific heat of water vapor at constant pressure		1952 J deg ⁻¹ kg ⁻¹
	Specific heat of water vapor at constant volume		1463 J deg ⁻¹ kg ⁻¹
	Specific heat of liquid water at 0°C		4218 J deg ⁻¹ kg ⁻¹
	Specific heat of ice at 0°C		2106 J deg ⁻¹ kg ⁻¹
	Latent heat of vaporization at 0°C		2.500 × 10 ⁶ J kg ⁻¹
	Latent heat of vaporization at 100°C		2.25 × 10 ⁶ J kg ⁻¹
	Latent heat of fusion at 0°C		3.34 × 10 ⁵ J kg ⁻¹

SOME OTHER SYMBOLS

symbol	units	name
g	m s^{-2}	gravitational acceleration
p	$\text{hPa}=100 \text{ Pa}$	pressure
T	K	temperature
T_d	K	dewpoint
T_w	K	wet-bulb temperature
z	m	height
Z	m	geopotential height
α	$\text{m}^3 \text{ kg}^{-1}$	specific volume
ρ	kg m^{-3}	air density
e	hPa	vapor pressure
r	kg kg^{-1}	mixing ratio
q	kg kg^{-1}	specific humidity
e_s	hPa	saturation vapor pressure
r_s	kg kg^{-1}	saturation mixing ratio
q_s	kg kg^{-1}	saturation specific humidity
θ	K	potential temperature
θ_e	K	equivalent potential temperature
θ_e^*	K	saturated equivalent potential temperature
θ_w	K	wet-bulb potential temperature
N	s^{-1}	Brunt-Vaisalla frequency
N_s	s^{-1}	moist Brunt-Vaisalla frequency
P	J kg^{-1}	convective available potential energy

The skew T diagram, and atmospheric stability

Note: The UCAR MetEd (Universities Corporation for Atmospheric Research Meteorological Education) group recently developed a nice online module called “Skew T mastery” (<http://www.meted.ucar.edu/mesoprim/skewt/>), which introduces both the skew T aerological diagram and the concept of static stability. Their graphic are superb. The notes below were used as one source for the development of this module. I encourage you to study this module, as the graphic illustrations will help you understand a complex diagram and the stability concepts.

1. The aerological diagram

i. Radiosondes

The observational information that is routinely examined in weather forecasting is presented commonly in two formats:

- surface and upper-level maps of pressure (or geopotential height) as well as temperature, wind, and humidity
- vertical profiles of temperature, humidity, and wind.

It is the latter type that is discussed here. The most common source of information for vertical structure still is the radiosonde instrument, although in the last few years remote sensing profiling systems have become the main source of upper-level data for numerical weather prediction. These include wind profilers and satellite-based multispectral sounders.

Radiosondes carried aloft by a balloon and are in communication with the ground via a radiotransmitter. They are released nearly simultaneously all over the world, typically twice a day. Especially in winter, in the midlatitude belt, a radiosonde may drift over a horizontal distance on the order of 100 km during its ascent through the troposphere. Nevertheless, for practical purposes the ascent generally is considered to be vertical; this assumption is based on the high degree of stratification the atmosphere typically exhibits.

ii. Hydrostatic balance; the hypsometric equation

The local vertical structure of the troposphere can be displayed in temperature- height (T-z) diagrams. However, this type of diagram is not commonly used, because on such a diagram the range of slopes of typical tropospheric profiles is not very wide, and mainly because the height is not an appropriate variable. Atmospheric pressure (p) is a better variable. That is because pressure (rather than height) is proportional to air *mass*, and therefore it can be used directly in the derivation of atmospheric properties such as energy (per unit mass). This pressure is the hydrostatic pressure. One beautiful characteristic of the atmosphere is that *hydrostatic balance* is very generally valid. Exceptions are rather local, e.g. in the vicinity of strong buoyancy forcing or extreme shear, as occurs near thunderstorms or steep terrain.

Hydrostatic balance states that the (downward) gravity force is exactly balanced by the (upward) pressure gradient force. Written per unit mass, this force balance is:

$$-\frac{1}{\rho} \frac{\partial p}{\partial z} = g \quad (1)$$

Another relation that generally applies to our atmosphere is the *ideal gas law*,

$$p = nR^*T \quad (2)$$

where n is the number of kilomoles per unit volume V (m^3) and R^* the universal gas constant.

Defining $R = R^*/M$, with M the average molecular weight of air¹,

$$p = \rho RT$$

since $nM = \rho$. This equation is the ideal gas law in a form commonly used in atmospheric science.

More correctly, we need to include the effect of variable water vapor concentrations in the air on the

air density. We define the *mixing ratio* r as $r = \frac{m_v}{m_d}$, where m_v is the mass of water vapor and m_d

the mass of dry air. Then the *virtual temperature* $T_v \equiv T(1 + 0.608r)$ needs to be used in the ideal gas law², so

$$\boxed{p = \rho RT_v} \quad (3)$$

Plugging (3) into (1) to eliminate ρ :

$$-\frac{1}{p} \frac{\partial p}{\partial z} = \frac{g}{RT_v} \quad (4)$$

If the atmosphere is isothermal, i.e. $T_v = T_o$ is constant, then (4) can be integrated from sea level ($z=0$) to any height z :

$$z = H \ln\left(\frac{p_o}{p}\right) \quad (5)$$

where z is the height above sea level, and p_o the sea level pressure. $H = \frac{RT_o}{g} = 29.3T_o$ is the *scale*

height. Assuming an average tropospheric temperature of 0°C , $H = 8$ km. The factor H is the e-folding depth of the atmosphere (every 8 km, the pressure drops by a factor of 2.7). Equation (5) (or (5')) in the footnote) is the simplest form of the *hypso-metric equation*³. Converted to

¹ The molecular weight M is expressed relative to the weight of one hydrogen atom. Dry air in the homosphere (below 100 km) has $M_d = 28.97$; water vapor has $M_v = 18.016$. One kilomole of hydrogen atoms corresponds to 1 kg, and to $6.022 \cdot 10^{26}$ atoms (Avogadro's number).

² This is derived as follows: the total pressure is the sum of the partial pressures due to dry air (p_d) and water vapor (e). Applying the ideal gas law to both:

$$p = p_d + e = \left(\frac{m_d}{M_d} + \frac{m_v}{M_v}\right) \frac{R^*T}{V} = \left(\frac{m_d}{m_d + m_v} + \frac{M_d m_v}{M_v (m_d + m_v)}\right) \rho RT \cong \left(1 - r + \frac{r}{\varepsilon} (1 - r)\right) \rho RT = \rho RT_v$$

where it is assumed that $m_v \ll m_d$. Note that $\frac{M_v}{M_d} = 0.622 \equiv \varepsilon$.

³ If the atmosphere is not isothermal, one can still integrate (4) approximately, assuming an average temperature. For instance, to calculate the depth δz of a layer between two pressure levels, p_1 and p_2 , p_2 being above p_1 , take the average temperature T_m and, as in (5),

$$p = p_o \exp\left(-\frac{z}{H}\right)$$

the hypsometric equation implies that pressure drops off exponentially with height. Equation (5) indicates how height can be calculated from pressure. In fact, that is how height is calculated from radiosonde data, although most operational radiosondes carry a GPS location-finding device nowadays. The GPS system also allows better determination of upper-level winds, as compared to the old signal tracking system.

iii. Aerological diagrams

The various aerological diagrams used by different weather service offices around the world all use pressure (or a function of pressure) as one of the coordinates. Aerological diagrams are alternatively referred to as *thermodynamic* or *pseudo-adiabatic* diagrams; the term pseudo-adiabatic arises from the use of the diagram to display moist adiabatic⁴ vertical motions. In doing so, the latent heat released by freezing and the accumulation of condensation/sublimation products are not taken into account, and therefore, these motions are referred to as pseudo-adiabatic. For our purpose, this is accurate enough.

Aerological diagrams are overwhelmingly complex at first glance, because of the large number of lines in different directions. They all consist of five types of lines: isobars, isotherms, saturated mixing ratio lines, dry adiabats (lines of constant θ), and saturated adiabats (lines of constant θ_e)⁵. Up to three types of lines can be straight on any diagram.

In addition to these 5 standard lines, 2 variable lines are plotted, i.e. the variation of temperature and dewpoint with height. These lines will be referred to as the ELR (environmental lapse rate) and DLR (dewpoint lapse rate), respectively. The term “environment” is used to distinguish it from a “parcel” of air that moves vertically under certain physical constraints. The basic constraints we assume is that the parcel⁶ does not mix mass or heat with the environment. Thus it moves up or down either in a *dry adiabatic* or a *moist adiabatic* fashion, as will be discussed later. In what follows it must be understood that under certain conditions parcels can move or be moved along certain *lines* in the diagram, but that under no circumstances an aerological diagram can be used to display a 2D *path* of a parcel.

$$\delta z = 29.27 T_m \ln\left(\frac{P_1}{P_2}\right) \quad (5')$$

Strictly speaking, the height z in (5) is the *geopotential* height Z , which integrates the effect of decreasing gravity with height above the surface:

$$Z = \frac{1}{g_o} \int_0^z g dz$$

where $g_o = 9.81 \text{ ms}^{-2}$, the global-mean gravitational acceleration at sea level. Within the troposphere, the difference between z and Z is less than 0.1%.

⁴ The term adiabatic refers to the fact that no heat is exchanged with the environment. See Section 2.4 below.

⁵ The variables θ and θ_e are introduced in Section 2.4.

⁶ More specifically, an air parcel is defined as a dimensionless, non-entraining bubble of air, whose pressure adjusts instantaneously to that of the ambient air thru which it rises or sinks.

A standard ELR, as defined by the International Civil Aviation Organization (ICAO), is shown on many diagrams. This temperature profile is entirely arbitrary, but is somewhat typical for the mid-latitude troposphere. The tropopause is the layer above the troposphere where the temperature changes little with height. From 11 km upwards, the ICAO profile is isothermal. So the ICAO tropopause is at 11 km. In reality, the height of the tropopause can vary from about 8 to 18 km.

Four different aerological diagrams are commonly used worldwide: emagrams, Stueve diagrams, skew T- log p diagrams, and tephigrams.

(a) **emagram**. Various European countries use an emagram (**Fig 1a**), which is very similar to a T-z plot: only the vertical axis is log p instead of height z. But log p is linearly related to height in a dry, isothermal atmosphere [see (5) above], so the vertical coordinate is essentially linear height.

(b) On **Stüve diagrams**, used in the USA, the vertical coordinate is $p^{\left(\frac{R_d}{c_p}\right)}$, and the horizontal coordinate is T, so the dry adiabats are straight lines (see section 2.4) (**Fig 1b**).

(c) A **skew T- log p diagram** is so-called because the vertical coordinate is linear in log p, and therefore approximately height, and because the isotherms are slanted (**Fig 1c**). You should have a skew T log p diagram (or *skew T* for short) in front of you. Use it continuously to test your understanding of this chapter.

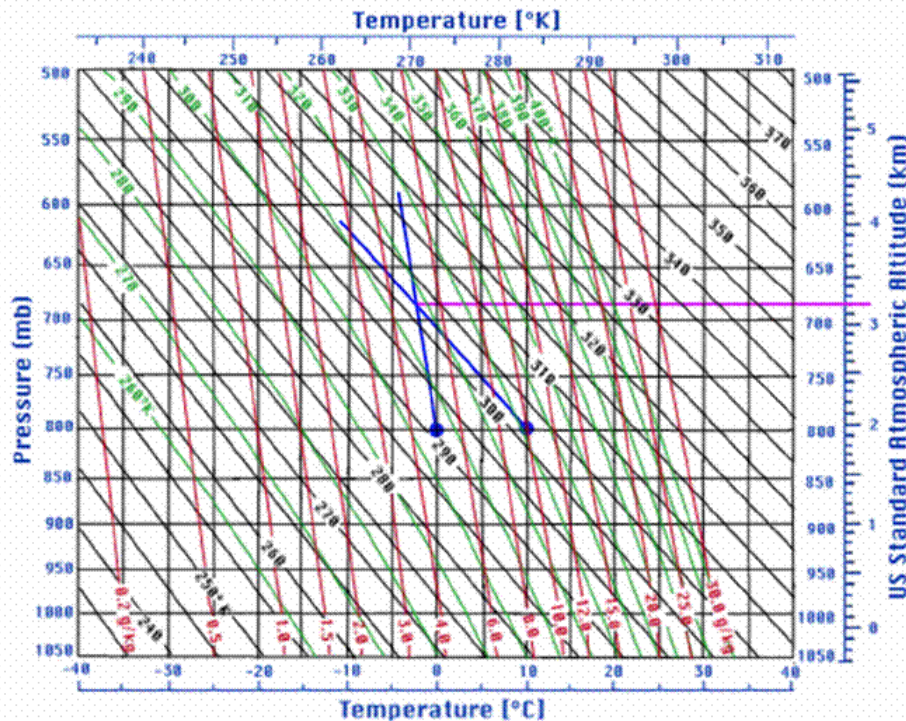


Fig 1a. An emagram

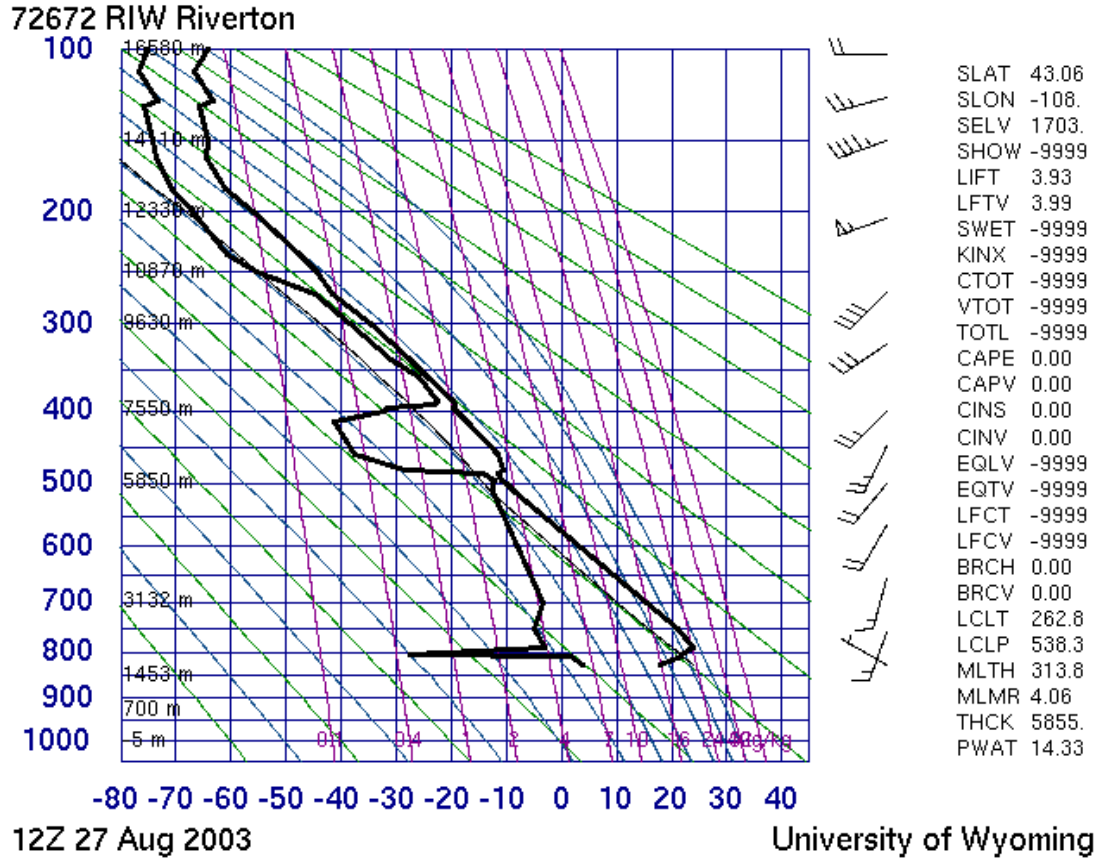


Fig 1b. A Stüve diagram (source: <http://weather.uwyo.edu>)

(d) **Tephigrams**, rotated by 45°, look very similar to skew T diagrams, but the base lines have a clear physical relationship. In the next section, the tephigram will be introduced, and in section 3 the diagram will be used to illustrate various concepts of parcel stability. Tephigrams, used in various Commonwealth countries (Canada, S. Africa, New Zealand), have horizontal and vertical coordinates of T and lnθ, respectively; i.e., the isotherms are vertical and the isentropes horizontal (hence tephigram, a contraction of T and φ, with entropy φ defined as $\phi = C_p \ln\theta + \text{constant}$) (**Fig 1d**). The tephigrams that you will be using in this class are rotated 45° clockwise so the vertical axis corresponds more or less with height.

A tephigram is superior to other diagrams in two ways. Firstly, only on a tephigram, a unit area corresponds with a unit amount of energy. This energy concept is important when estimating thunderstorm intensity, or the likelihood of convective initiation (CAPE and CIN, see later). On other diagrams, the concept of area=energy only applies approximately. Secondly, because the angle between isotherms and isentropes (90°) is larger than in any other diagram, variations in environmental lapse rate (ELR) can most easily be discerned on a tephigram

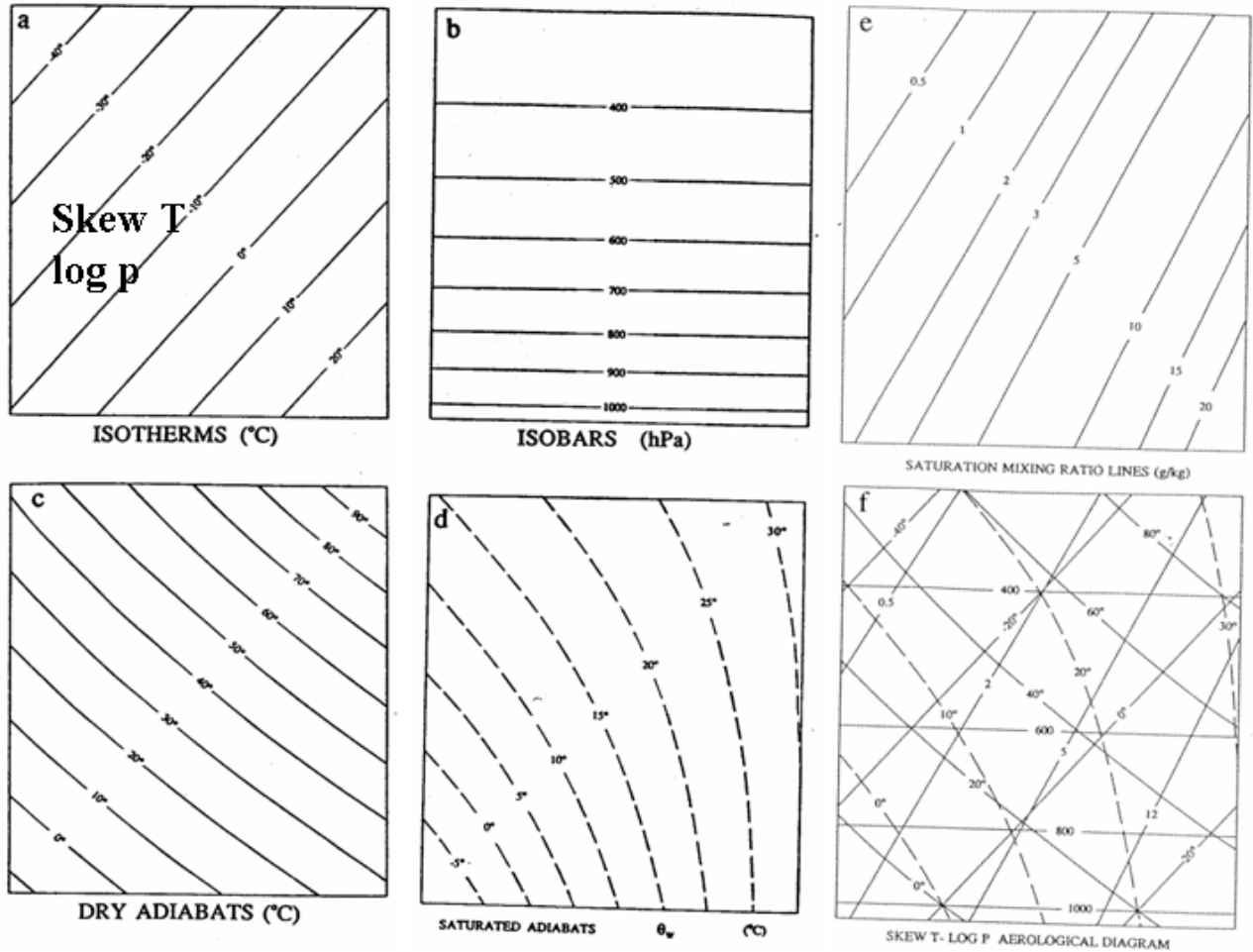


Fig 1c. Elements of a Skew T log p diagram. All lines are combined in the lower right diagram.

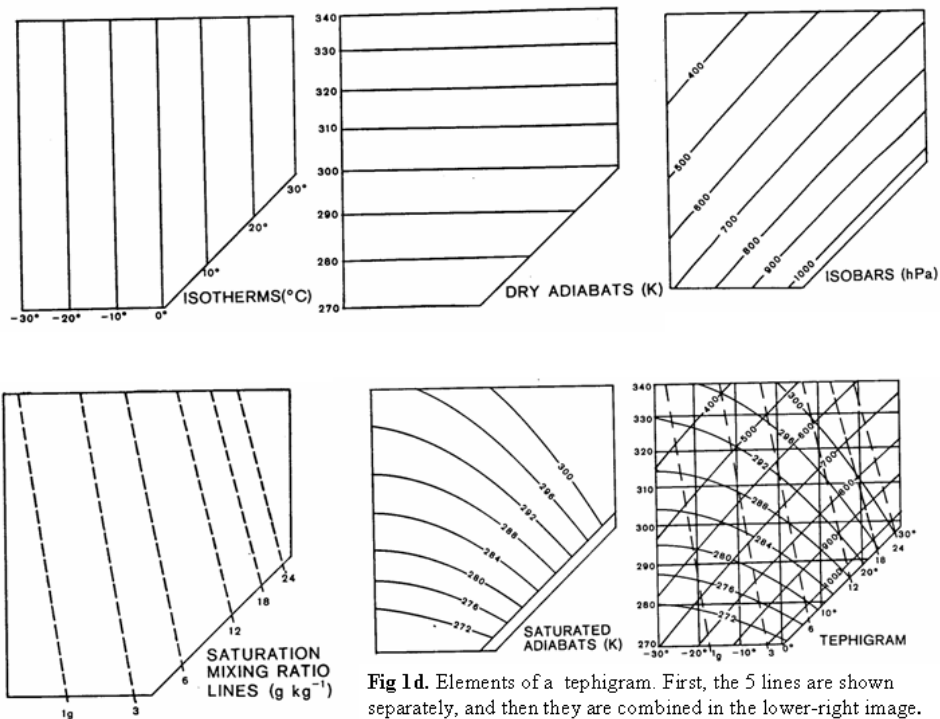


Fig 1d. Elements of a tephigram. First, the 5 lines are shown separately, and then they are combined in the lower-right image.

2. Skew T applications

The purpose of this section is to familiarize the reader with the use of the skew T, and to introduce some relevant concepts.

(i) The skew T diagram

The skew T consists of three sets of straight lines, isobars (horizontal), the isotherms (diagonal), and the saturation mixing ratio lines (steep diagonal) (Fig 1d). The dry and saturated adiabats are upward and downward convex resp.. The data from model output for Los Angeles at 22 UTC on 10 Jan 2011 have been plotted as two solid bold lines in Fig 2: the right-most one (red), the ELR, consists of temperature (T) data at various levels; and the one on the left (blue), the DLR, connects model output of the dewpoint (T_d) at the same levels. Because T_d is less than or equal to T, the DLR is always to the left of the ELR. Only when the air is saturated do the DLR and the ELR coincide.

It can be seen in Fig 2 that the temperature generally decreases with height, except in the lower stratosphere. Can you spot the tropopause? It is very well defined in this case, as a sharp kink in the ELR. The increase in temperature with height is referred to as an *inversion*. Sometimes, as in this case, a mid-tropospheric stable layer exists. In this case this stable layer is saturated, indicating mid-level clouds. The winds are plotted on the right, as barbs (one full barb is 10 kts, one triangle is 50 kts). Not the vigorous winds in the lower stratosphere.

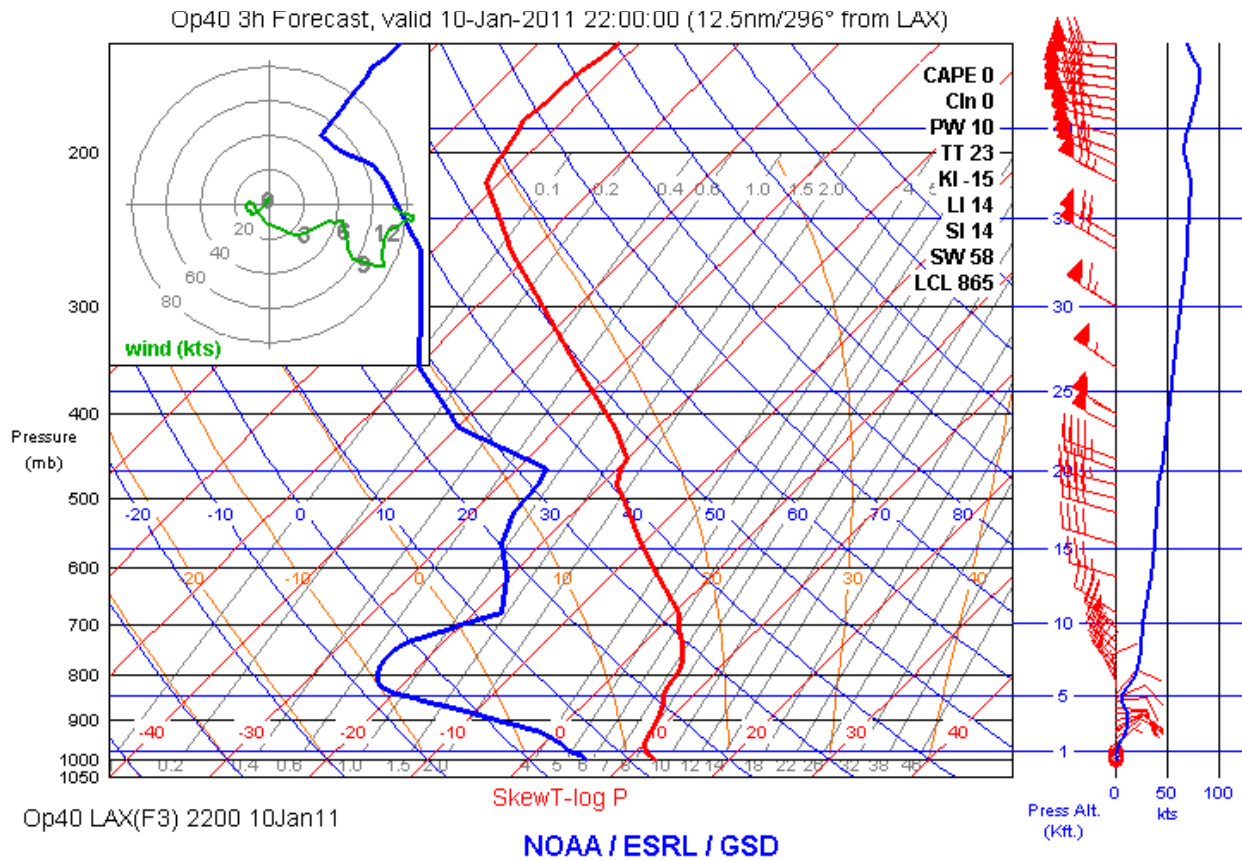


Fig 2. A sample sounding plotted on a skew T, for Los Angeles (LAX) on 10 Jan 2011 (source: <http://rucsoundings.noaa.gov/>)

(ii) *Determination of moisture parameters*

One of the useful aspects of the aerological diagram is that moisture parameters can be determined fairly simply.

- **Specific humidity** (q): the amount of water vapor (kg) relative to the amount of air (kg) - *read or interpolate the value of the saturation specific humidity line which cuts the DLR at the required pressure* (Fig 3 a).
- **Saturation specific humidity** (q_s) - *read or interpolate the value of the specific humidity line which cuts the ELR at the required pressure.*
- **Relative humidity** (RH) - *read or interpolate values of q and q_s as above and use*

$$RH = 100 \frac{q}{q_s} = 100 \frac{r}{r_s} \quad (\%) \quad (6)$$

where r (r_s) is the (saturation) mixing ratio, defined as the (saturation) amount of water vapor (kg) relative to the amount of dry air (kg). In other words,

$$q = \frac{m_v}{m_h} \quad \text{while} \quad r = \frac{m_v}{m_d} \quad (7)$$

where m_d is the mass of the dry air, m_v the mass of the water vapor, and m_h the mass of the humid air, so $m_h = m_d + m_v$. Therefore, and since in the troposphere $m_v \ll m_d$,

$$q = \frac{r}{1+r} \approx r(1-r) \approx r \quad (8)$$

Therefore the specific humidity lines are commonly referred to as *mixing ratio lines*. For all physical applications (e.g. the first law of thermodynamics, equations of motion), we shall work per unit mass of air (m_h), and thus use q .

- **Vapor pressure** (e) - *from the DLR at the required pressure, follow an isotherm to its intersection with the 622 hPa isobar. Read or interpolate the mixing ratio at this point and this value equals the vapor pressure in hPa* (Fig 3 b).

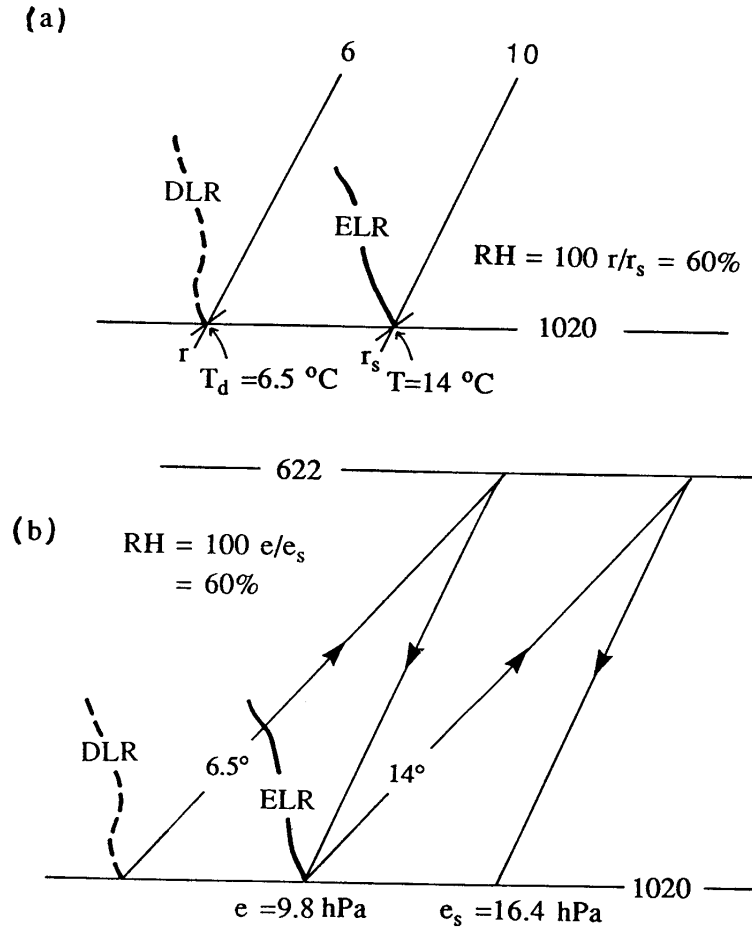


Fig. 3: Determination (at an arbitrary pressure level p) of (a) mixing ratio, saturation mixing ratio and relative humidity; (b) vapour pressure, saturation vapour pressure and relative humidity.

• **Saturation vapor pressure (e_s)** - from the ELR at the required pressure, follow an isotherm to its intersection with the 622 hPa isobar. Then do as for vapor pressure above.

What is the magic of 622 hPa? In the determination of e_s , you do not really lift or descend a parcel to the 622 hPa level. You only graphically apply the relation⁷

⁷ This relation results from the definition of q , and the use of the ideal gas law (2) for the partial pressures of water vapor (e) and air (p) within the same volume V . Start with the definition for q (see eqn 7). Now the n_v , the number of

kilomoles of water vapor per unit volume V is $n_v = \frac{m_v}{VM_v}$, and similarly $n_h = \frac{m_h}{VM_d}$ for the full atmospheric

composition. The molecular weights M for water vapor and total air have been defined before. Taking the ratios of the total air pressure p over the water vapor partial pressure e and applying the ideal gas law (2) for both:

$$\frac{p}{e} = \frac{n_h R^* T}{n_v R^* T} = \frac{n_h}{n_v} = \frac{m_h M_v}{m_v M_d} = 0.622 \frac{1}{q}$$

So, defining $\epsilon = 0.622$,

$$q = \epsilon \frac{e}{p} \tag{9}$$

$$q_{s,p,T} = 0.622 \frac{e_{s,p,T}}{p} \quad (q \text{ in kg/kg; } e_s \text{ and } p \text{ in hPa}) \quad (9)$$

Then, at 622 hPa, $q_{s,622,T} = e_{s,622,T}/1000$ and $e_{s,622,T} = e_{s,p,T}$ if the temperature T is the same, since e_s depends only on temperature (that is why you follow an isotherm). The same technique is used in the determination of e (above), but now T is replaced by T_d .

(iii) *Lifting condensation level (LCL)*

The LCL (expressed in hPa) is the level to which an air parcel needs to be lifted in order to become saturated. The distance from the surface to the LCL is proportional to the dewpoint depression ($T - T_d$) at the reference level. By definition of the dewpoint T_d , the mixing ratio of air equals the saturation mixing ratio at the air's dewpoint:

$$r = r_{s,T_d} \quad (10)$$

You should convince yourself that the mixing ratio of unsaturated air does not change in the event of vertical displacements; that is because the mixing ratio (or the specific humidity) is a ratio of two masses, which both decrease proportionally in a unit volume when the air expands. As long as a parcel is unsaturated, it will rise dry adiabatically. Therefore, the LCL can be determined as the intersection between the dry adiabat (the line which follows a dry adiabatic lapse rate, or DALR) through the reference temperature and the saturation mixing ratio line through the reference dewpoint (Fig 4).

In the context of what follows you will note that the LCL is unrelated to atmospheric stability. The LCL is of most relevance when surface air is forced to rise, e.g. over a mountain. The LCL is typically calculated for a parcel originally positioned at the ground surface, although it can be applied at any level. When there is good evidence that the clouds are produced by lifting from the surface (e.g. fair-weather cumuli in the convective boundary layer), then the height of the cloud base, H_{LCL} (in km, measured from the ground), can be estimated from surface observations. All you need is T and T_d at the surface, as follows:

$$H_{LCL} = \frac{T - T_d}{\Gamma_d - \Gamma_{T_d}} = \frac{T - T_d}{8} \quad (\text{km}) \quad (11)$$

where Γ_d is the dry adiabatic lapse rate (10 K km^{-1} , see below) and Γ_{T_d} the dewpoint lapse rate (2 K km^{-1}) if the mixing ratio is conserved. The temperature at the cloud base can then be estimated as

$$T_{\text{cloudbase}} = T_{\text{surface}} - 10H_{LCL} \quad (\text{K or } ^\circ\text{C}) \quad (12)$$

(iv) *(Dry) potential temperature*

To describe the (static) energy of a parcel of air, it is not sufficient to know its temperature. For instance, a parcel over a desert may be very hot during the day, e.g. $35 \text{ }^\circ\text{C}$ (95°F); when this parcel rises buoyantly to (say) 5 km high, it is quite cold (if the parcel remains unsaturated, it will be about $-15 \text{ }^\circ\text{C}$ or 5°F). Conversely, if a parcel of air over a tropical forest, at $35 \text{ }^\circ\text{C}$, buoyantly rises to the same height, it will be much warmer, because it received latent heat from the condensed water vapor. Typically, the atmosphere is stably stratified, with a lapse rate of about 6.5 K km^{-1} , so at 5

km the environment would be 2.5°C in this scenario. The dry parcel clearly would be colder than the environment, but the jungle air might be warmer. Generally, rising air is anomalously cool, compared to the ambient air at the same level. And vice versa, a parcel subsiding from the middle troposphere is typically anomalously warm. In other words, the troposphere normally is stably stratified. This will be discussed further in Section 3. To understand that section, we need to be familiar with the concept of *potential temperature*. In general, a potential temperature is a pseudo-temperature, which is conserved in the absence of external heat sources. Potential temperature describes the static energy of a parcel.

• **Potential temperature (θ) (Fig 4)** - The potential temperature is the temperature that a parcel of air would have if it were moved dry adiabatically to a pressure of 1000 hPa. Assuming no diabatic sources or sinks, the first law of thermodynamics is:

$$mc_v dT_v + pdV = 0$$

or, per unit mass (m),

$$c_v dT_v + pd\alpha = 0 \quad (13)$$

with $\alpha \equiv \frac{1}{\rho} = \frac{V}{m}$, where V is the (variable) volume of the unit mass. Using the ideal gas law (3),

(13) can be transformed to

$$c_p dT_v - \alpha dp = 0 \quad (14)$$

where $c_p = c_v + R$ (the relation of Mayer)⁸. In atmospheric thermodynamics, the first law is usually expressed the form of (14). To solve this differential equation, the variables need to be separated. Using the ideal gas law again to eliminate α ,

$$\frac{dT_v}{T_v} - \frac{R}{c_p} \frac{dp}{p} = 0 \quad (15)$$

So with the boundary condition $T_v = \theta$ at $p = p_0 = 1000$ hPa, the solution to (15) is that

$$\theta \equiv T_v \left(\frac{p_0}{p} \right)^{R/c_p} \quad (16)$$

is constant, or that

$$\frac{d\theta}{\theta} = d \ln \theta = 0 \quad (17)$$

⁸ c_p , c_v , and R are constants, to a very good approximation.

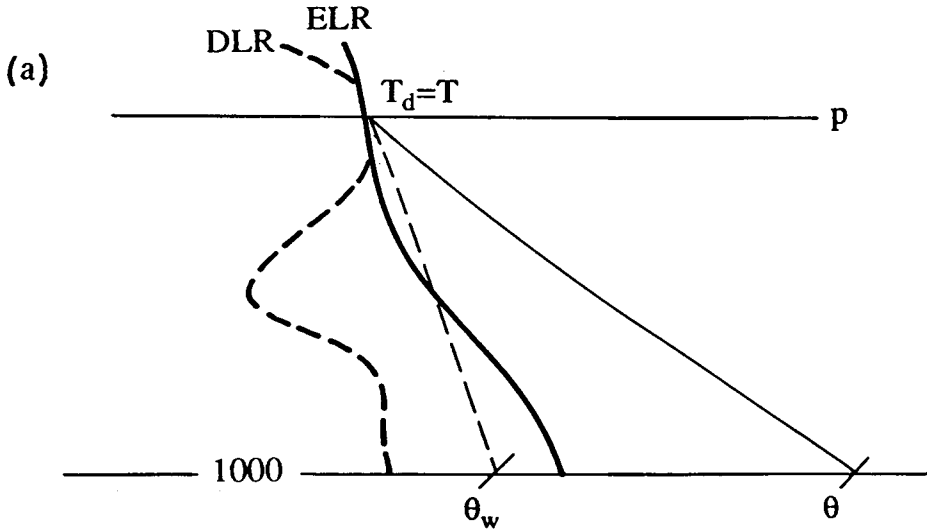


Fig 4a. Determination of potential temperature θ and wet-bulb potential temperature θ_w for a saturated parcel of air.

θ is defined as the (virtual) potential temperature⁹, and clearly it is conserved, independent of its dynamics, as long as no diabatic heating/cooling affects the air mass. Note that θ is closely related to the (dry) static energy s ,

$$s \equiv c_p T_v + gz \quad (\text{J kg}^{-1})$$

Using the hydrostatic equation (1), and going back from (17) to (15), one can show that only diabatic processes change dry static energy¹⁰:

$$ds = c_p T_v d \ln \theta$$

The vertical axis of the original tephigram is $\ln \theta$, and the horizontal axis T (Fig 1d). The integral of a surface area on the tephigram, $\int x dy$ or $\int T d \ln \theta$, therefore is proportional to an amount of dry static energy s .

⁹ In most textbooks θ is defined as $\theta \equiv T_v \left(\frac{p_0}{p}\right)^{R/c_p}$ and $\theta_v = \theta(1 + 0.608r)$. For simplicity, we define θ with the

virtual temperature correction included. This correction ($\theta_v - \theta$) can be 2K in magnitude, in warm humid conditions.

¹⁰ Note that other textbooks, such as Holton (2004), define entropy dS as $dS = c_p d \ln \theta$ (we use phi or ϕ for entropy). Entropy is not quite the same as dry static energy.

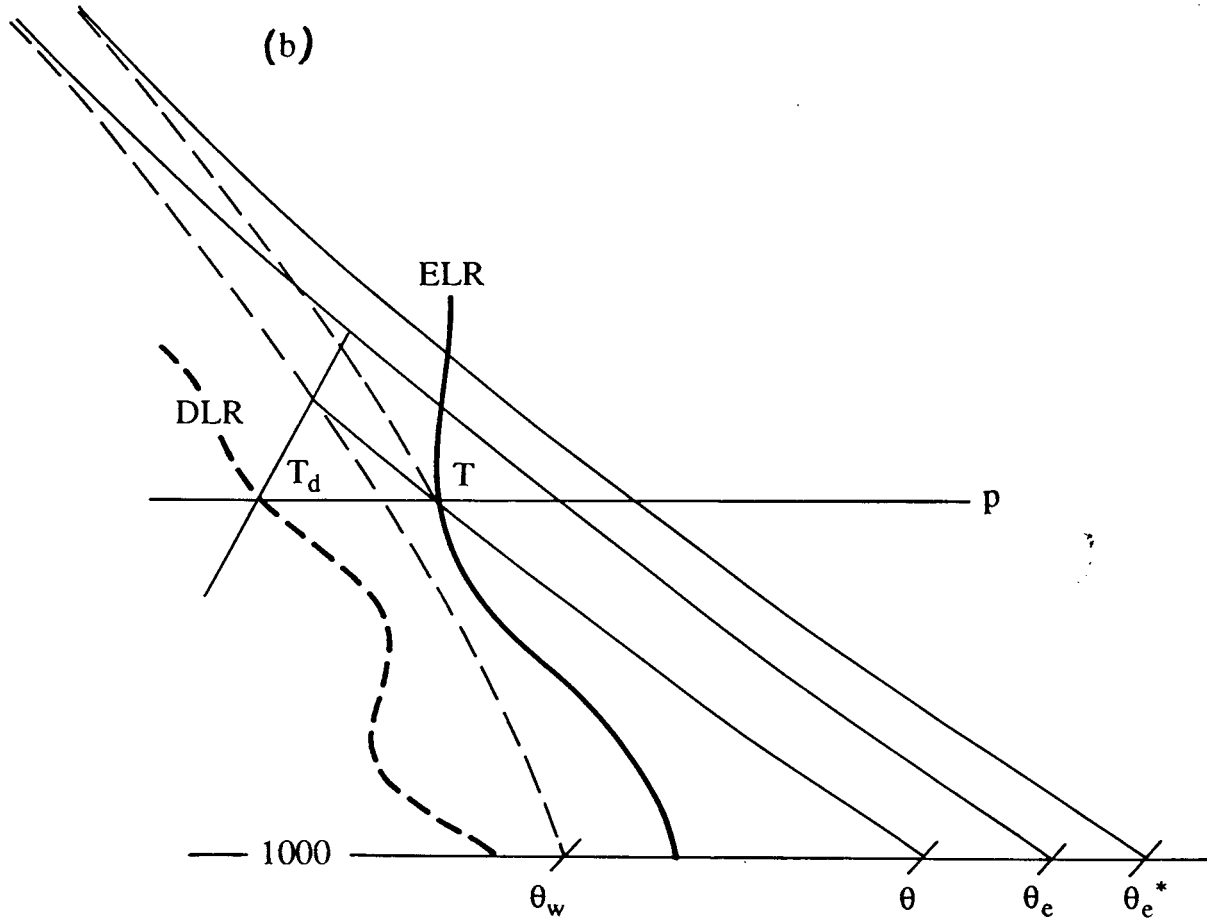


Fig 4b. Determination of θ , θ_w , equivalent potential temperature θ_e , and saturated equivalent potential temperature θ_e^* , for a dry parcel. Distinguish the ELR and DLR (bold solid and dashed lines) from the dry and moist adiabats (thin solid and dashed lines, respectively).

θ is determined graphically by reading or interpolating the value of the dry adiabat corresponding to the required temperature and pressure. In other words, just as T is the variable that determines an isotherm, so is θ the variable that quantifies a *dry adiabatic lapse rate* DALR. An alternative procedure is to follow the dry adiabat to 1000 hPa from a point with specified temperature and pressure. The potential temperature then is given by the isotherm at 1000 hPa. On your skew T, θ is expressed in °C, but in equations θ should be expressed in Kelvin, as is T .

The derivation of θ allows an estimation of the DALR. Starting from (15), use the hydrostatic equation (1) to substitute dp :

$$\frac{dT_v}{T_v} + \frac{g\rho R}{pc_p} dz = 0$$

or, using the ideal gas law (3),

$$\frac{dT_v}{dz} = -\frac{g}{c_p}$$

so the DALR , Γ_d , is

$$\Gamma_d \equiv -\left(\frac{dT_v}{dz}\right)_{DA} = \frac{g}{c_p} \quad (18)$$

To a close approximation, the DALR Γ_d is 10 K km^{-1} .

(v) *Moist potential temperatures*

• **Wet-bulb potential temperature** (θ_w). The wet-bulb potential temperature of a saturated parcel is the temperature that it would have if it were moved moist adiabatically to a pressure of 1000 hPa (Fig 4a). The procedure for finding θ_w is to read or interpolate the value of the saturated adiabat corresponding to the required temperature and pressure. In other words, θ_w is the variable that quantifies a *saturated adiabatic lapse rate* (SALR) (on your skew T, it is labelled in °C).

Alternatively, one can find θ_w on an aerological diagram as the temperature of a saturated parcel moved moist adiabatically to 1000 hPa. For a non-saturated (“dry”) parcel, it is harder to determine θ_w (Fig 4b). One follows a DALR upwards till it intersects with the saturation mixing ratio line through the dewpoint. Then θ_w can be determined by interpolation between the nearest SALR’s. θ_w is referred to as the wet-bulb potential temperature because the SALR also determines the wet-bulb temperature T_w at the reference pressure level (Normand’s proposition - see further).

Mathematically, θ_w can be calculated as follows:

$$\theta_w \equiv \theta \cdot \exp\left[\frac{L(q_s(\theta_w, p_o) - q)}{c_p T}\right] \quad (19)$$

where $q_s(\theta_w, p_o)$ is the saturation specific humidity at a temperature of θ_w at $p_o=1000 \text{ hPa}$. Clearly this is a non-linear, recursive equation that can only be solved with an iterative method. Therefore θ_w is used in aerological diagrams mostly, and is rarely calculated. For quantitative purposes, the equivalent potential temperature is generally used, as it has the same physical properties in θ_w , but is easier to compute.

• **Equivalent potential temperature** (θ_e) (Fig 4 b) - The equivalent potential temperature of a parcel is the temperature it would reach at 1000 hPa if it were first lifted high enough that it would not retain any water. Again, the only diabatic heat source is evaporation/condensation. This heat source balances the left hand side of (14):

$$c_p dT_v - \alpha dp = -Ldq \quad (20)$$

where L is the latent heat of vaporization, and q the specific humidity.

Again we use the ideal gas law (as in (14)) to transform (20) to:

$$\frac{dT_v}{T_v} - \frac{R}{c_p} \frac{dp}{p} = -\frac{L}{c_p T_v} dq$$

or

$$\frac{d\theta}{\theta} = -\frac{L}{c_p T_v} dq \quad (21)$$

Now T_v is a variable, and strictly speaking L is a function of temperature¹¹. However, a scaling analysis shows that the change of the right hand side of (21) into a total differential involves a typical error of a few percent¹², so we can write

$$d \ln \theta = -d\left(\frac{Lq}{c_p T}\right) \quad (22)$$

This differential equation can be solved with the boundary condition that $\theta = \theta_e$ when $q = 0$. Then (22) can be written as

$$\frac{d\theta_e}{\theta_e} = 0$$

where θ_e (the *equivalent potential temperature*) is defined as

$$\theta_e \equiv \theta_e \cdot e^{\left(\frac{Lq}{c_p T_e}\right)} \quad (23)$$

θ_e has the same characteristics as θ_w ¹³. In fact, θ_e is an alternative variable to quantify the SALR's. The difference is that θ_e is independent of the reference level, and therefore θ_e is physically more meaningful. Note that θ_e depends on both temperature (T) and humidity (q). Convince yourself that the more water vapor there is in the air (which is only possible at high temperature), the more water vapor is condensed upon lifting, and therefore, the more the latent heating in a rising parcel offsets the cooling due to expansion. Therefore, a SALR is smaller than the DALR, and the difference is larger at higher temperature (verify this on your aerological diagram).

Notice first that θ_e (or θ_w) of a parcel is (very close to being) conserved under both dry and saturated conditions. To see this, examine eqn (23): when the air is non-saturated, both θ and q are conserved in updrafts and downdrafts (the conservation of q follows from definition (17)), so ignoring any change in T in the exponent in (23), θ_e is conserved. And when the air is saturated ($q = q_s$ where q_s is the saturation specific humidity), the derivation to (22) shows that θ_e is conserved, as long as no ice forms. Therefore, θ_e is a good “identifier” of an air mass. The θ_e of a parcel can only be changed by external heat sources (radiation or diffusion).

Notice also that θ_e (or θ_w) is not conserved when freezing (or melting) occurs, in which case energy is released (or required). A typical liquid water content of a convective updraft rising above the freezing level is 1 g kg^{-1} , which upon freezing gives the updraft a buoyancy of merely 0.33 K above the θ_e value. The effect of the freezing of droplets is small compared to the effect of condensation, since the latent heat of fusion is much smaller (7.5 times) than the latent heat of vaporization. For open systems, a conservative potential temperature variable that includes the effect of freezing/melting does not exist.

Next, note that θ_e is closely related to the (*moist*) *static energy* of a system, h . Defining $h \equiv s + Lq$, it follows from the definition of the dry static energy s and (22) that, at least approximately,

¹¹ Approximately, $L = 2500 \{1000 - (T - 273.15)\} \text{ J kg}^{-1}$

¹² In the tropical boundary layer, the error can be as large as 20%. This assumption is the largest weakness in the use of θ_e as a conserved variable.

¹³ Specifically, θ_w is derived from the first law of thermodynamics as well. θ_w can be calculated from (21), but with the boundary condition that $T = \theta_w$ when $p = p_0$ and $q = q_r$, where q_r is the specific humidity at the reference level.

$$dh = c_p T_v d \ln \theta_e$$

So h is conserved when θ_e is conserved. In fact, because the approximation from (20) to (21) is not needed for h , h is even better conserved. And a more complete static energy could be defined that includes the effect of fusion/melting. The reason why θ_e is used more commonly, I believe, is simply because meteorologists rather think in terms of degrees than joules. Still, θ_e is a good measure of the potential energy content of the air, part of which can be converted to the kinetic energy of deep-convective updrafts.

• **Moist adiabatic lapse rate.** The derivation of θ_e makes it possible to estimate the value of the SALR. Starting from (20), with (1):

$$\frac{1}{T_v} \frac{dT_v}{dz} + \frac{R}{c_p} \frac{\rho g}{p} = -\frac{L}{c_p T_v} \frac{dq}{dz} \quad (24a)$$

When calculating the SALR, the air is assumed saturated, so $q = q_s$. According to (9), $q_s = 0.622 \frac{e_s}{p}$,

$$\frac{dq_s}{q_s} = \frac{de_s}{e_s} - \frac{dp}{p} \quad (24b)$$

According to the Clausius-Clapeyron equation,

$$\frac{de_s}{e_s dT_v} = \frac{\varepsilon L}{RT_v^2}$$

e_s depends only on T_v , so $\frac{de_s}{e_s} = \frac{1}{e_s} \frac{de_s}{dT_v} dT_v$. Then (24b) becomes:

$$\frac{dq_s}{q_s} = \frac{\varepsilon L}{RT_v^2} dT_v - \frac{dp}{p}$$

and using hydrostatic balance (1) and the ideal gas law (3), this can be written as:

$$\frac{dq_s}{dz} = \frac{q_s \varepsilon L}{RT_v^2} \frac{dT_v}{dz} + \frac{q_s g}{RT_v} \quad (24c)$$

Plugging (24c) into (24a)

$$\frac{dT_v}{dz} + \frac{g}{c_p} = -\frac{\varepsilon L^2 q_s}{R c_p T_v^2} \frac{dT_v}{dz} + \frac{q_s g L}{R c_p T_v}$$

where we used the ideal gas law (3). So, with the definition of the DALR Γ_d , the SALR Γ_s is:

$$\Gamma_s \equiv -\left(\frac{dT_v}{dz}\right)_{SA} = \frac{\Gamma_d \left(1 + \frac{q_s L}{RT_v}\right)}{1 + \frac{\varepsilon L^2 q_s}{R c_p T_v^2}} \quad (24d)$$

It follows from (24d) that Γ_s approaches Γ_d as the air dries out ($q_s \rightarrow 0$), which happens when $T \rightarrow 0$. Thus at very low temperatures the SALR=DALR (10 K km^{-1}), i.e. the moist adiabats become

parallel to the dry adiabats. It can be shown from (24d) that for all temperatures $\Gamma_s < \Gamma_d$ and $\frac{d\Gamma_s}{dT} < 0$

. This can be seen on a skew T: the moist adiabats are more vertical (closer to the isotherms) than the dry adiabats, and the difference between moist and dry adiabats is larger when the temperature is higher.

• **Saturated equivalent potential temperature (θ_e^*)**(Fig 4b) - The saturated equivalent potential temperature is the θ_e that a parcel would have if it were saturated. So:

$$\theta_e^* \equiv \theta_e e^{\left(\frac{Lq_s}{c_p T_v}\right)} \tag{25}$$

Naturally θ_e^* is larger than θ_e unless the parcel was already saturated. θ_e^* is determined the same way as θ_e but it is assumed that the parcel is saturated from the reference pressure. θ_e^* *does not characterize the air*, it only indicates the extra energy a parcel would have if it were saturated.

(vi) *Normand's rule*

It was Sir C.W.B. Normand who in 1934 first propositioned that the LCL of an air parcel is located on an aerological diagram at a triple line intersection of the dry adiabat through the reference (dry-bulb) temperature (T), the saturation mixing ratio line through the reference dewpoint (T_d), and the saturated adiabat through the wet-bulb temperature (T_w) (**Fig 5**). The intersection of the first two lines at the LCL is precisely the definition of the LCL (see section 2.3). It is the third intersecting line which is surprising, especially since the measurement of T_w seems so instrument-dependent (e.g., aspiration of psychrometer, quality of wet cloth). The correspondence can be understood by inverting the ascent: a parcel descending from the LCL to the reference level normally reaches the temperature T; however, if the parcel were supplied with sufficient moisture (e.g., by ‘coating’ it with a wet cloth), it would descend moist adiabatically to a temperature T_w . The temperature difference ($T - T_w$) at the reference level is solely due to latent heat release from the available moisture (the wet cloth); the same is true for the temperature difference between dry-bulb and wet-bulb thermometers on a psychrometer. Normand's rule can be used to calculate any of the variables (T, T_w , T_d , LCL, and θ_w) if any two of them are known.

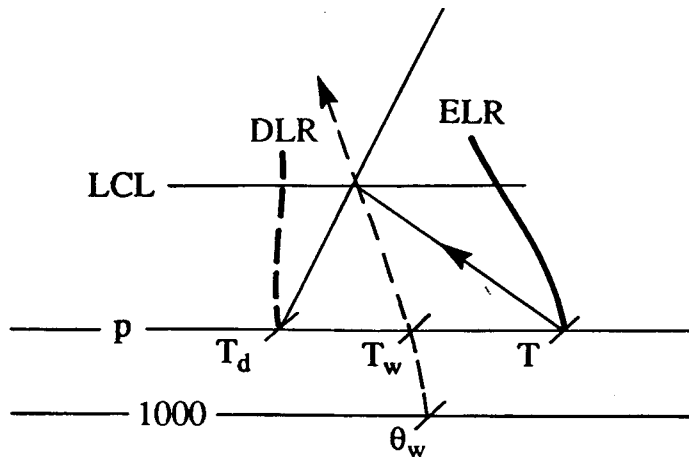


Fig 5. Determination of the lifting condensation level (LCL) and Normand's proposition. The arrow indicates a parcel's ascent.

(vii) *Convection condensation level (CCL)*

The CCL (expressed in hPa) is the level at which a parcel, rising buoyantly from the surface by surface heating will become saturated. The *convection temperature* is the temperature to which the air needs to be heated at the ground, for convection to develop at the CCL. Notice the difference between the CCL and the LCL; in the latter case the surface air is lifted, not heated.

You are well aware that in the warm season a clear morning is followed by the sudden appearance of shallow cumulus clouds. These clouds typically have a flat base and shallow depth. They may grow to become cumulonimbi; in any event, they disappear towards the evening. Such clouds are due to convection driven by surface sensible (and latent) heat flux. One can make a good prediction of the cloud base (CCL) and the time of onset of these clouds with the aid of an atmospheric sounding taken in the morning, because the diurnal change in surface temperature usually is much greater than the change in dewpoint and ELR aloft. This is most valid in summer when there is little large scale variation. The CCL and convection temperature is then determined as follows (**Fig 6**): the CCL is at the level where the saturation mixing ratio line through the surface dewpoint intersects with the ELR; the convection temperature (T_c) is the temperature at the surface that connects dry adiabatically to the CCL. Then if you know the typical rate of change of surface temperature in the morning hours, you can also predict the time of onset of convection.

To understand this, increase the surface temperature gradually, and draw a dry adiabat between the new surface temperature and the ELR. Then ask yourself whether the parcel reached saturation along the DALR trace. The parcel will only reach saturation if its DALR trace intersects with the saturation mixing ratio line (through the surface dewpoint) before it intersects the ELR. The reason why the lapse rate in the lowest layers assumes a DALR, when the surface is heated, will become more clear when you read about stability (Section 3). Such changes in boundary-layer temperature really happen: the *convective boundary layer* is well-mixed (near-uniform θ and q) and gradually deepens during the morning hours, until about local solar noon.

A corollary of the definition of the CCL is that the LCL is below the CCL, except when the surface temperature reaches the convection temperature, in which case the LCL is at the CCL (**Fig 7**).

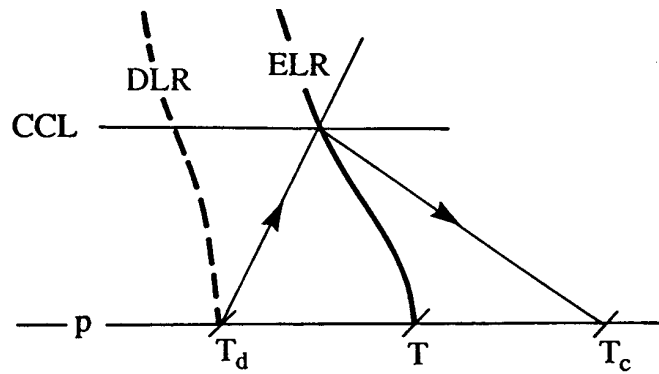


Fig. 6: Determination of the convection condensation level (CCL) and the convection temperature (T_c).

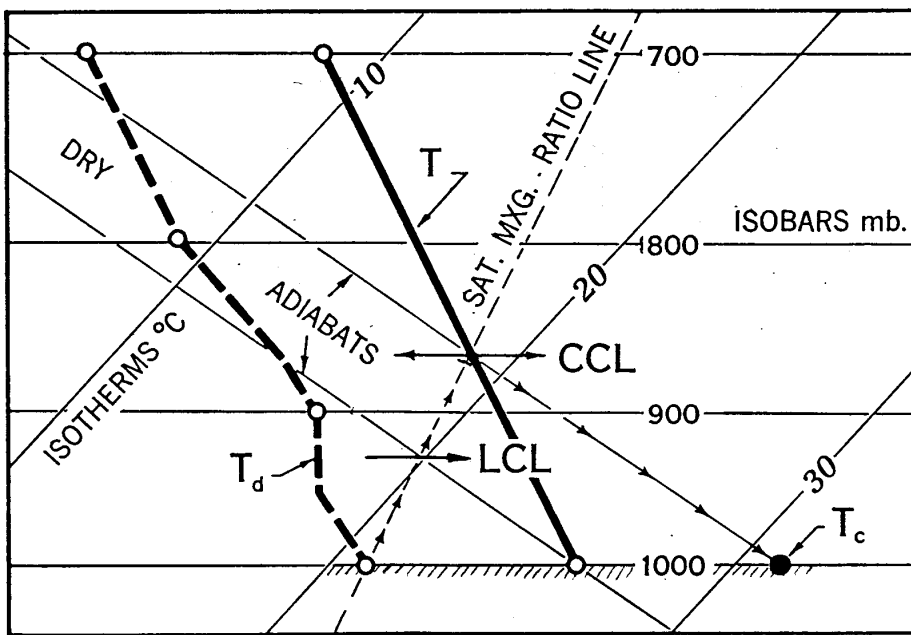


Fig. 7: The relation between CCL and LCL (source: Manual of Meteorology, 1975).

(viii) *Some other applications*

(a) **Thickness (δz)**

The thickness of a layer can obviously be approximated from the aerological diagram without any data: the height corresponding to any pressure level is given on the left hand side, in both km and 1000's of feet. However, this pressure/height relation is only valid for the ICAO standard atmosphere. For any real ELR, the pressure/height relation is somewhat different. Not only is the exact height of a pressure level an important meteorological datum; it is at least as important in atmospheric dynamics to know the thickness, that is the height difference between two pressure levels.

The thickness can be approximated by a graphical method, the equal area method (**Fig 8a**). In order to calculate the thickness between pressure levels p and p_0 (e.g. 500 and 1000 hPa), given the ELR,

from A to B, a dry adiabat XY is drawn through AB in such a way that the area XAO equals the area YO B. The temperature difference between the points X and Y then defines ΔT , from which the thickness is derived as:

$$\delta z = \frac{\Delta T}{\Gamma_d} \quad (m) \quad (26)$$

The key to this argument is that the adiabatic layer XY has the same mean temperature, and hence the same thickness, as the layer AB.

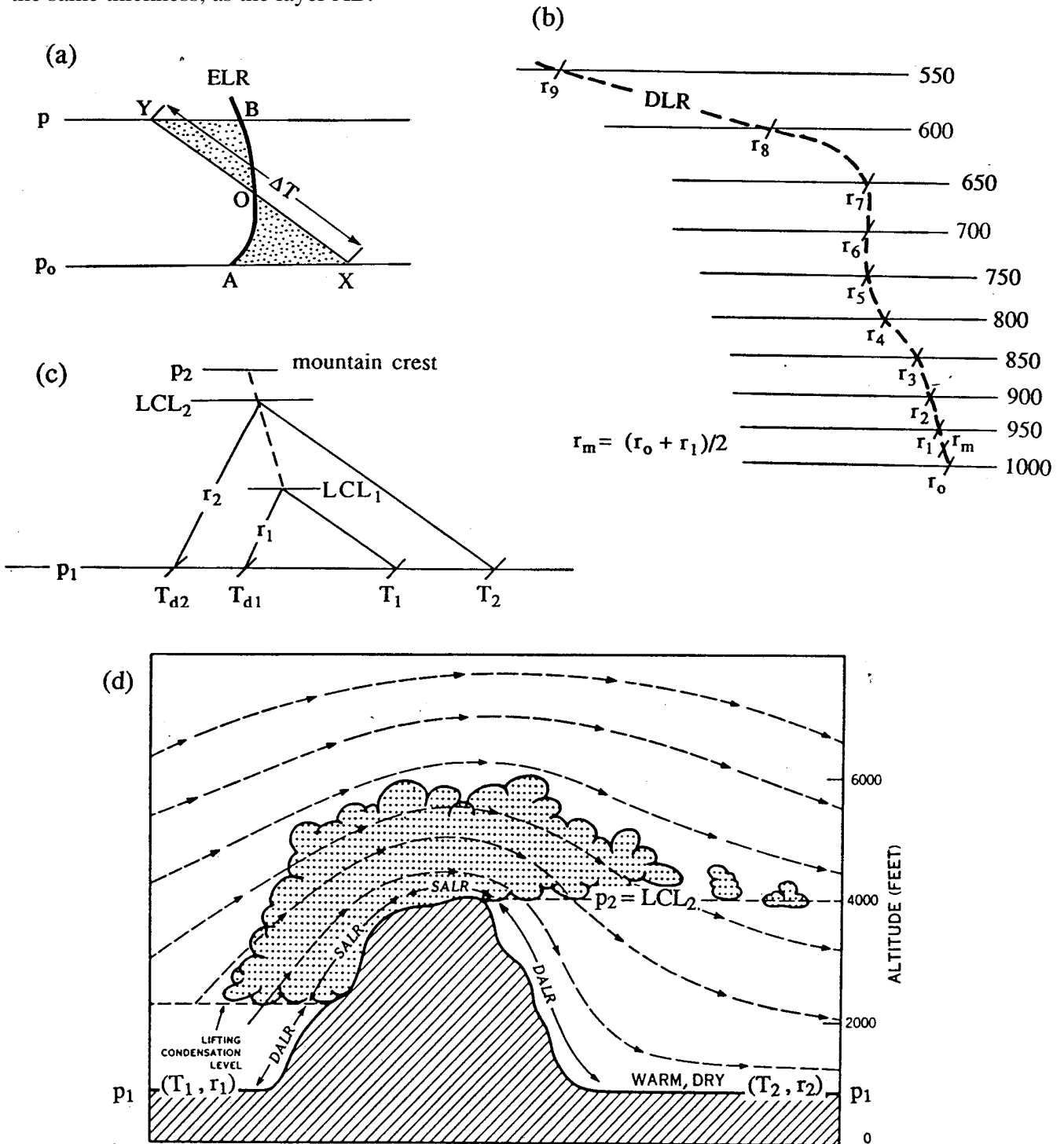


Fig. 8

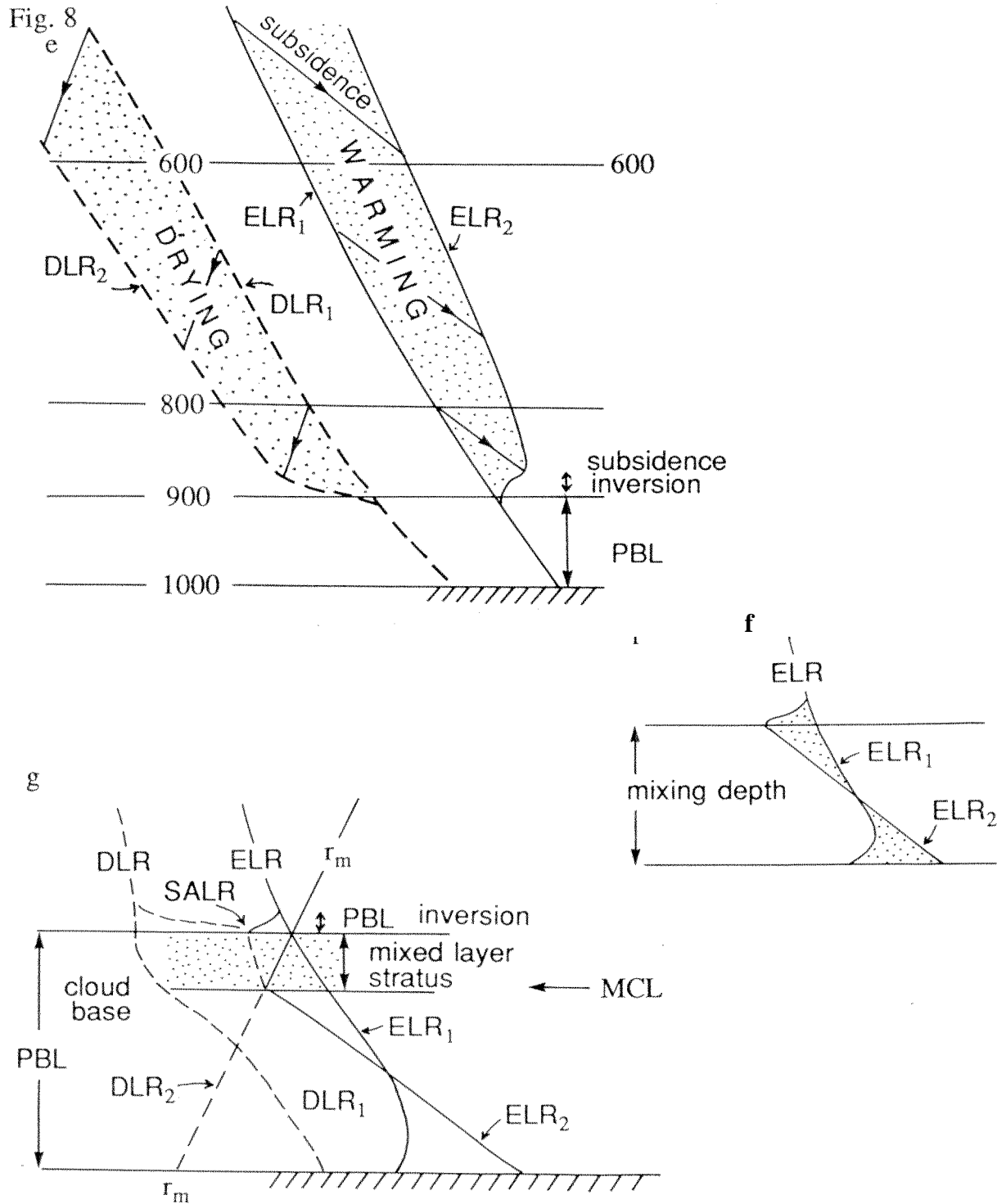


Fig 8. Determination of (a) thickness by the equal area method; (b) precipitable water; (c) and (d) the Föhn effect; (e) warming by subsidence; (f) the effect of shear-forced turbulence on the ELR; (g) mixed layer stratus and the mixing condensation level (MCL). Subscript (1) refers to the initial state, (2) to the final state. For the Föhn effect, the initial state is on the upwind side, and the final state on the downwind (lee) side of the mountain, at the same height.

The thickness can be estimated mathematically using the hypsometric equation [see equation (5') in footnote 3]:

$$\delta z = 29.27 T_m \ln\left(\frac{P_o}{p}\right) \quad (\text{m}) \quad (5')$$

where T_m is the mean temperature for the layer,

$$T_m = \frac{T_A + T_B}{2} \quad (\text{K}) \quad (27)$$

For instance, the thickness of the 1000 - 500 hPa layer can be computed as:

$$\delta z = 20.3 T_m \quad (\text{m}) \quad (28)$$

(b) Precipitable water (PW)

The *precipitable water* is the total amount of water that is contained as water vapor in an atmospheric column. The global longterm average precipitable water is 26 mm, but there are considerable regional variations. The precipitable water of a sounding is an important parameter for the understanding and prediction of rainfall rates and precipitation totals. Since $\Delta p/g$ is the mass of air in a unit area of a column of depth Δz (see (1), over a finite layer), the precipitable water is:

$$PW = \frac{1}{\rho_l} \sum \bar{r}_i \frac{\Delta p}{g} \quad (\text{m}) \quad (29)$$

where \bar{r} (kg/kg) is the mean mixing ratio for a layer, ρ_l the density of water, and the summation is over all layers $i=0 \dots \infty$ of the sounding (see **Fig 8b**). In practice, when the pressure increment Δp is 50 hPa, the precipitable water PW' (in mm) is simply a weighted sum of the mixing ratios r' (in g kg^{-1}) as follows:

$$PW' = \frac{r_o'}{4} + \sum \frac{\bar{r}_i'}{2} \quad (\text{mm}) \quad (30)$$

where r_o' is the mixing ratio at the surface (g kg^{-1}).

(c) Föhn effect:

The term Föhn (or Chinook) is used for the arrival of warmer and drier air at the lee side of a mountain range. Its cause, the moist adiabatic ascent on the windward side and the dry adiabatic subsidence on the leeside, can be illustrated on a tephigram (**Fig 8c**). Air with properties T_1 , T_{d1} , and r_1 at level p_1 on the windward side is lifted orographically to p_2 (**Fig 8d**). The ascent is dry adiabatic up to the LCL_1 and moist adiabatic higher up. A quantity $\delta r = r_1 - r_2$ is lost through precipitation. Some cloud water (or ice) is carried with the air over the mountain, and evaporates in the leeside subsidence, but for tall mountains that fraction is usually negligibly small. Therefore, the lifting condensation level at the leeside (LCL_2) is only just below the mountain crest (p_2). The subsidence from there is entirely dry adiabatic. Note that both $T_2 > T_1$ and $T_{d2} < T_{d1}$, so typically the relative humidity is very low on the leeside (**Fig 8d**).

(d) Large scale subsidence

Large scale subsidence (**Fig 8e**) occurs for instance in the subtropical highs and to the rear of cold fronts. Because the ELR is virtually never as large as the DALR (i.e. the atmosphere is naturally stably stratified), the dry-adiabatically subsiding air undergoes real warming. At the same time, the mixing ratio of the subsiding air is conserved, so the relative humidity of the air decreases.

Subsidence normally does not proceed all the way to ground level, not just because of continuity, but also because of surface fluxes and shear-induced mixing (turbulence) in the planetary boundary layer (PBL). The interface between large-scale subsidence and PBL mixing leads to an extremely stable interface, often an inversion. Such *subsidence inversion* is recognized especially by the low relative humidity aloft (**Fig 8e**). Widespread subsidence is common in subtropical areas, in the descending branch of the Hadley cell. The subsidence inversion in these areas is referred to as the trade wind inversion, and coincides with the top of the marine PBL.

(e) Turbulent mixing in the PBL

In a well-mixed layer, isolated from other layers of air and from heat sources, the lapse rate will be close to adiabatic (**Fig 8f**). Because prior to mixing the lapse rate is normally smaller (more vertical), an inversion may develop at the boundary to the next layer. This inversion is referred to in general as a *turbulence inversion*. This process is important in the PBL, where mixing is caused by wind shear and the interaction of wind with the (rough) ground surface. The equal area method based on the ELR is used to find the appropriate DALR of the mixed layer (**Fig 8f**). Notice that the upper half is being cooled in the process. The mixing ratio of the mixed air is constant and is determined by the equal area method based on the DLR (**Fig 8f**). When the air is moist enough, then the upper section of the layer may be saturated (**Fig 8g**), giving rise to a thin layer of stratus clouds. In this case, the equal area method is more difficult to apply, because the top section of the new ELR (ELR₂) follows a SALR. The equal area method may also be applied to find a representative mixing ratio (r_m) after turbulent mixing. Observe that DLR follows the saturation mixing ratio line r_m up to the cloud base (**Fig 8g**).

When a cloud layer is due to internal mixing (typically in the PBL), the cloud base is referred to as the mixing condensation level (MCL). It is important to differentiate the MCL from the CCL and the LCL. In the formation of a MCL, heat is exchanged between the upper and lower half of the layer. In the case of the CCL, heat is added to the PBL. And in the case of the LCL, the air below the cloud base is cooled by lifting. In reality, clouds are rarely formed by one single process, for instance during the daytime, over land, PBL mixing occurs both by convection, sustained by surface heat fluxes, and by mechanical (shear-induced) mixing. In order to predict the cloud base and cloud type from an aerological diagram, one needs to estimate first which process will be dominant.

(f) Conservative variables

Some atmospheric variables remain constant when the air undergoes a change due to some process. Such variable is said to be conservative with respect to (or *for*) such process. For instance, as pointed out before, the mixing ratio is conserved for subsidence or lifting, as long the air is not saturated. Conservative properties are particularly useful in tracing the origin of air and in the classification of different air masses. In this context, the wet-bulb potential temperature θ_w is a useful variable because it is conserved for both condensation/ evaporation and uplift/ subsidence.

And relative humidity, RH, or temperature, T, are poor variables for air mass identification (**Table 1**).

The conservation properties of the variables listed in Table 1 are all simplifications of the energy conservation principle of static air. As you will see in an Atmospheric Dynamics course (e.g. ATSC 4031), there are other conservation principles for air in motion, e.g. the conservation of momentum and of angular momentum. There are conservative variables derived from a combination of static and dynamic principles, in particular potential vorticity. These variables are of extreme value in the identification and characterization of an air mass, not only its (thermodynamic) state, i.e. the temperature, pressure, density and humidity, but also its dynamic state, i.e. the 3-D velocity and vorticity.

Table 1: Processes for which certain properties of the atmosphere are conserved.

property	This variable is conservative for the process of ...				
	radiational heating/cooling	evaporation/condensation	ascent/descent	turbulent mixing of	
				heat	water vapor
T	-	-	-	-	+*
T_d	+*	-	-	+*	-
T_w	-	+	-	-	-
θ	-	-	+*	-	+*
θ_e or θ_w	-	+	+	-	-
q	+	-	+*	+	-
RH	-	-	-	-	-

* provided that condensation does not occur.

3. Static stability

(i) *The concept of stability*

The concept of (local) stability is an important one in meteorology. In general, the word stability is used to indicate a condition of equilibrium. A system is stable if it resists changes, like a ball in a depression. No matter in which direction the ball is moved over a small distance, when released it will roll back into the centre of the depression, and it will oscillate back and forth, until it eventually stalls. A ball on a hill, however, is unstably located. To some extent, a parcel of air behaves exactly like this ball.

Certain processes act to make the atmosphere unstable; then the atmosphere reacts dynamically and exchanges potential energy into kinetic energy, in order to restore equilibrium. For instance, the development and evolution of extratropical fronts is believed to be no more than an atmospheric response to a destabilizing process; this process is essentially the atmospheric heating over the equatorial region and the cooling over the poles. Here, we are only concerned with static stability, i.e. no pre-existing motion is required, unlike other types of atmospheric instability, like baroclinic or symmetric instability. The restoring atmospheric motion in a statically stable atmosphere is strictly vertical. When the atmosphere is statically unstable, then any vertical departure leads to buoyancy. This buoyancy leads to vertical accelerations away from the point of origin. In the context of this chapter, stability is used interchangeably with static stability.

The most general application of stability is in synoptic-scale weather forecasting; stability concepts are used, for instance, in the identification of

- unstable conditions suitable for the formation of convective clouds, from fair weather cumuli to severe thunderstorms;
- a variety of stable conditions:
 - o warm or cold fronts aloft, recognized by an elevated inversion, often capped by a saturated layer of air, indicating uplift, unlike a subsidence inversion, which is;
 - o subsidence inversions, capped by a dry layer (unlike frontal inversions), which indicates descent of tropospheric air; they are associated with low-level highs or ridges (see further);
 - o turbulence inversions which develop as a result of frictional mixing, typically close to the surface (see further);
 - o radiation inversions which form on clear nights when the ground cools more rapidly than the air above. In urban locations these conditions can lead to the trapping of pollutants emitted by industrial sources and motor vehicles, thereby affecting the quality of the air.

Therefore, a knowledge of the concepts of stability and how the thermal structure of the atmosphere changes in space and time is needed to understand changing weather conditions.

(ii) *The parcel technique*

(a) **Stable, neutral and unstable**

The stability of any part of the atmosphere can be determined from its ELR and, in some conditions, its DLR. Perhaps the best way to explain how static stability can be determined is to disturb a dry (unsaturated) parcel of air in the hypothetical case of **Fig 9**.

Take a parcel of air at point P and lift it over a short distance. Assume that the parcel does not mix with the surrounding air and remains dry, so its vertical movement will be dry-adiabatic, i.e. upon rising its temperature will decrease at a rate of $1^\circ\text{C}/100\text{ m}$ (the DALR). It will, on Fig 9a, follow the DALR. Since the potential temperature (θ) of a dry air parcel is conserved, a parcel will follow a vertical line on a θ -z plot (Fig 9b). It is obvious, then, that if it is lifted, it will be colder than the environment (ELR) (Fig 9a). It follows from the equation of state (at constant pressure) that it must be denser, and hence heavier than the environment. Since the environment is in a state of hydrostatic equilibrium, the parcel must have a downward gravity force greater than the upward pressure gradient force. In other words, the parcel is negatively buoyant, and it sinks back to the point P. This displacement is illustrated in Figs. 9a and 9b.

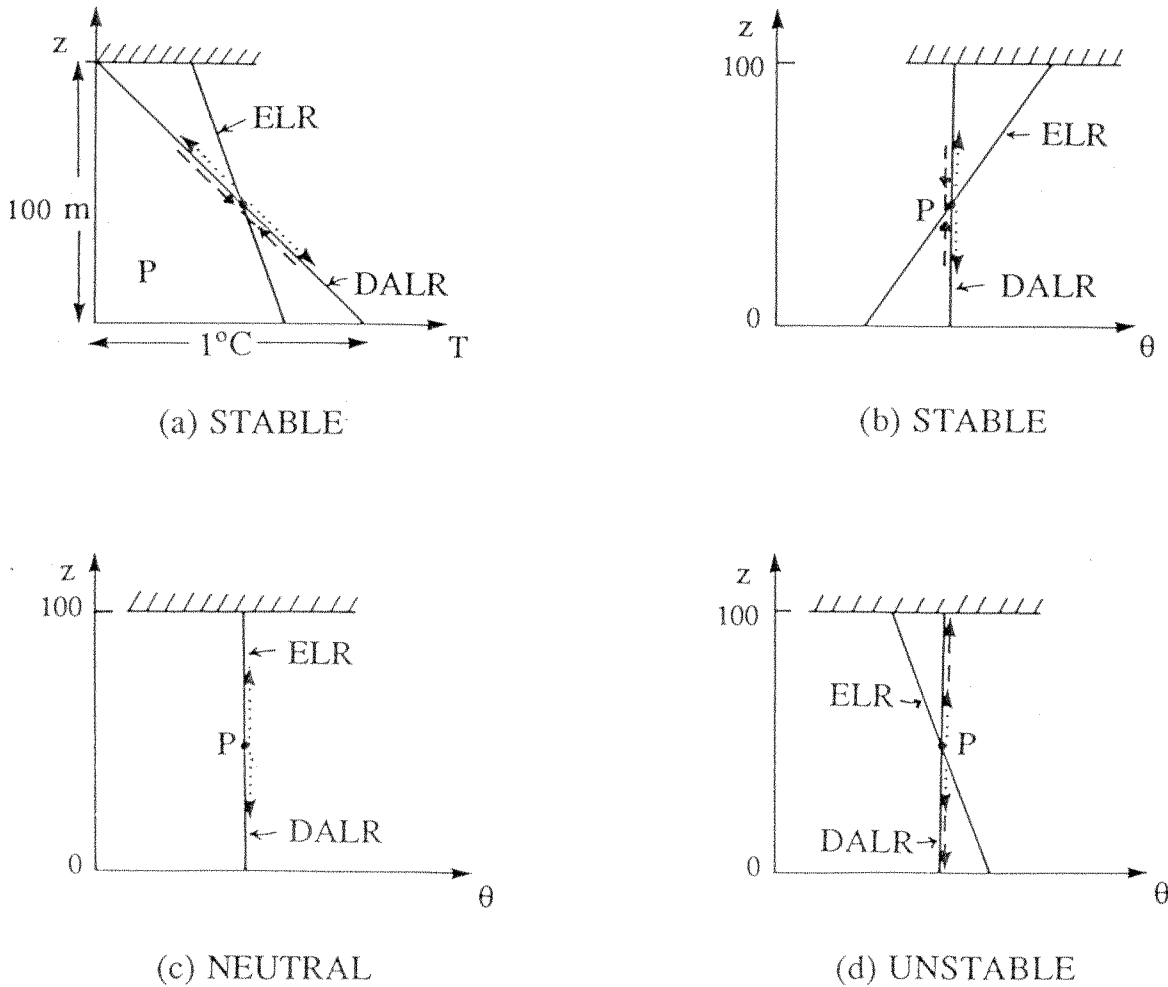


Fig 9. Local atmospheric stability for a dry parcel. (a) stable ELR on a T-z diagram; (b) ibidem, plotted on a θ -z diagram; (c) a neutral ELR; (d) an unstable ELR. The point of reference is P. The dotted arrow traces the initial displacement of a parcel. The dashed arrow shows the parcel's response.

A similar argument will show that if it is initially forced downward it will be warmer than the surroundings, and will experience an upward force and also will return to its initial position. Clearly, the ELR is stable in this case. In other words, a layer of air is said to be in local stable

equilibrium if, after any displacement of a parcel from its initial position, it experiences a force which returns it to that point. Compare this to the situation depicted in Fig 9c; in this case, the ELR is parallel to the DALR (that is a vertical line on a θ -z plot). An air parcel, whether lifted or subsided, will always be at the same temperature as the environment. The atmospheric profile is neutral in this case.

Finally, in Fig 9d, the ELR tilts to the left of the vertical on a θ -z plot. A parcel, when lifted from P, will be warmer than the environment, and it will continue to rise spontaneously. If the parcel were forced downward, it would have been colder than the environment, and it would have fallen further. This ELR is locally unstable.

Note that in a stable atmosphere, a perturbed parcel does not simply return to its original position. Instead, once perturbed, it will oscillate vertically around its original position, with a frequency (or oscillation rate) called the Brunt-Vaisalla frequency (after the names of a British and a Finnish meteorologist). The oscillation will only be damped by friction and mixing.

The movement of an air parcel can be compared with that of a ball on a non-level surface. A ball, pushed slightly sideways out of the centre of a depression, will converge in a damped oscillation towards the centre. If there were no friction, the ball would never stall. The frequency of the oscillation depends on the shape of the depression; deeper depressions have a higher frequency. Similarly, the oscillation frequency of an air parcel depends on atmospheric stability; the Brunt-Vaisalla frequency in an inversion is larger than that in a marginally stable layer.

The theory is as follows: assume that the environment is in hydrostatic balance,

$$\frac{d\bar{p}}{dz} = -\bar{\rho}g$$

where the over-bars refer to the basic state, which is a function of height z only. A parcel of air that is displaced vertically assumes the environmental pressure \bar{p} instantaneously (see footnote 5). It will conserve its potential temperature, which is $\bar{\theta}$ at height z , while the environment has a variable lapse rate $\frac{d\bar{\theta}}{dz}$. Then, at a finite displacement δz , the parcel has a potential temperature $\bar{\theta}$, while the

environment has a potential temperature $\bar{\theta} + \frac{d\bar{\theta}}{dz} \delta z$. Let $\delta\theta$ be the difference in potential

temperatures between parcel and environment. Then $\delta\theta = -\frac{d\bar{\theta}}{dz} \delta z$. From (3),(13) and (15), it follows that:

$$\frac{d\theta}{\theta} = -\frac{d\rho}{\rho} + \frac{c_v}{c_p} \frac{dp}{p} \quad (31)$$

So the difference in potential temperatures between parcel and environment at height $z + \delta z$ is:

$$\delta\theta = -\bar{\theta} \frac{\delta\rho}{\bar{\rho}} \quad (32)$$

since the pressure adjusts instantaneously. $\delta\rho$ is the difference in density between parcel and environment. It is assumed that $\delta\rho \ll \bar{\rho}$. Both $-g \frac{\delta\rho}{\bar{\rho}}$ and $g \frac{\delta\theta}{\bar{\theta}}$ are expressions of the buoyancy of an air parcel. The parcel's density is $\rho = \bar{\rho} + \delta\rho$. The vertical equation of motion is:

$$\frac{dw}{dt} = \frac{d^2\delta z}{dt^2} = -\frac{1}{\rho} \frac{dp}{dz} - g = -\frac{1}{\bar{\rho}} \frac{dp}{dz} - g + \frac{\delta\rho}{\bar{\rho}^2} \frac{dp}{dz} \quad (33a)$$

since the pressure perturbation is zero [hint: use: $\frac{1}{\bar{\rho} + \delta\rho} = \frac{1}{\bar{\rho}} \frac{1}{(1 + \frac{\delta\rho}{\bar{\rho}})} \cong \frac{1}{\bar{\rho}} (1 - \frac{\delta\rho}{\bar{\rho}})$]. Now use the

hydrostatic equation to obtain:

$$\frac{d^2\delta z}{dt^2} = -g \frac{\delta\rho}{\bar{\rho}} = g \frac{\delta\theta}{\bar{\theta}} = -\frac{g}{\bar{\theta}} \frac{d\bar{\theta}}{dz} \delta z \quad (33b)$$

So

$$y'' + N^2 y = 0 \quad (34)$$

where $y = \delta z$ and y'' is its second derivative with time t , and

$$N^2 = \frac{g}{\bar{\theta}} \frac{d\bar{\theta}}{dz}$$

is the square of the Brunt-Vaisalla frequency. The general solution of (34) is $y = Ae^{iNt}$ where A is a constant. Clearly, when $N^2 < 0$, the solution increases exponentially with height, i.e. the atmosphere is unstable. The criterion for static instability then is:

$$\boxed{\frac{d\bar{\theta}}{dz} < 0} \quad (35)$$

Usually, $N^2 > 0$, in which case the solution of (34) is oscillatory, and the oscillation has a period (called buoyancy period) of $\frac{2\pi}{N}$.

(b) Local and non-local stability

To carry on with the analogy, it is clear that a ball in a depression is stable. So far, we have assumed that any perturbation is infinitesimal, i.e. that the displacements are small. In other words, we have considered *local stability*. However, if a parcel were originally positioned on a high hill above the depression, it would, when released, roll down (a hill corresponds to an unstable ELR), roll through the depression and across the adjacent hill, and never return (**Fig 10**). Therefore, while a depression is locally stable (by definition), it is in the case of Fig 10 non-locally unstable. Non-local stability depends on the surroundings. Therefore, whenever in the real troposphere atmospheric stability is evaluated, the entire profile from ground to tropopause should be known. It is for this reason also that, to eliminate non-local effects, the ELR's analysed in Fig 9 are confined at the top and the bottom.

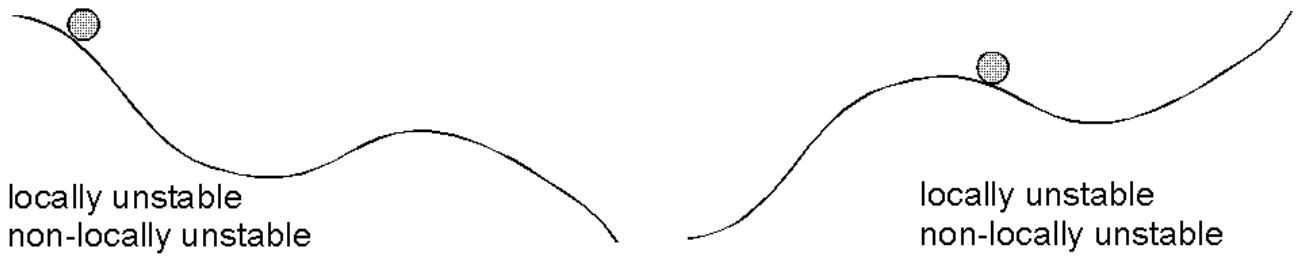


Fig 10. Local vs non-local instability.

To further illustrate the difference between local and non-local stability, consider **Fig 11**. From Figs 9b and 9d it is clear that when the ELR tilts to the right with height, it is (locally) stable, and that when it tilts to the left, it is (locally) unstable. A vertical ELR is (locally) neutral (Fig 9c). This can be verified in Fig 11a, which shows an arbitrary, unbounded ELR on a θ -z plot.

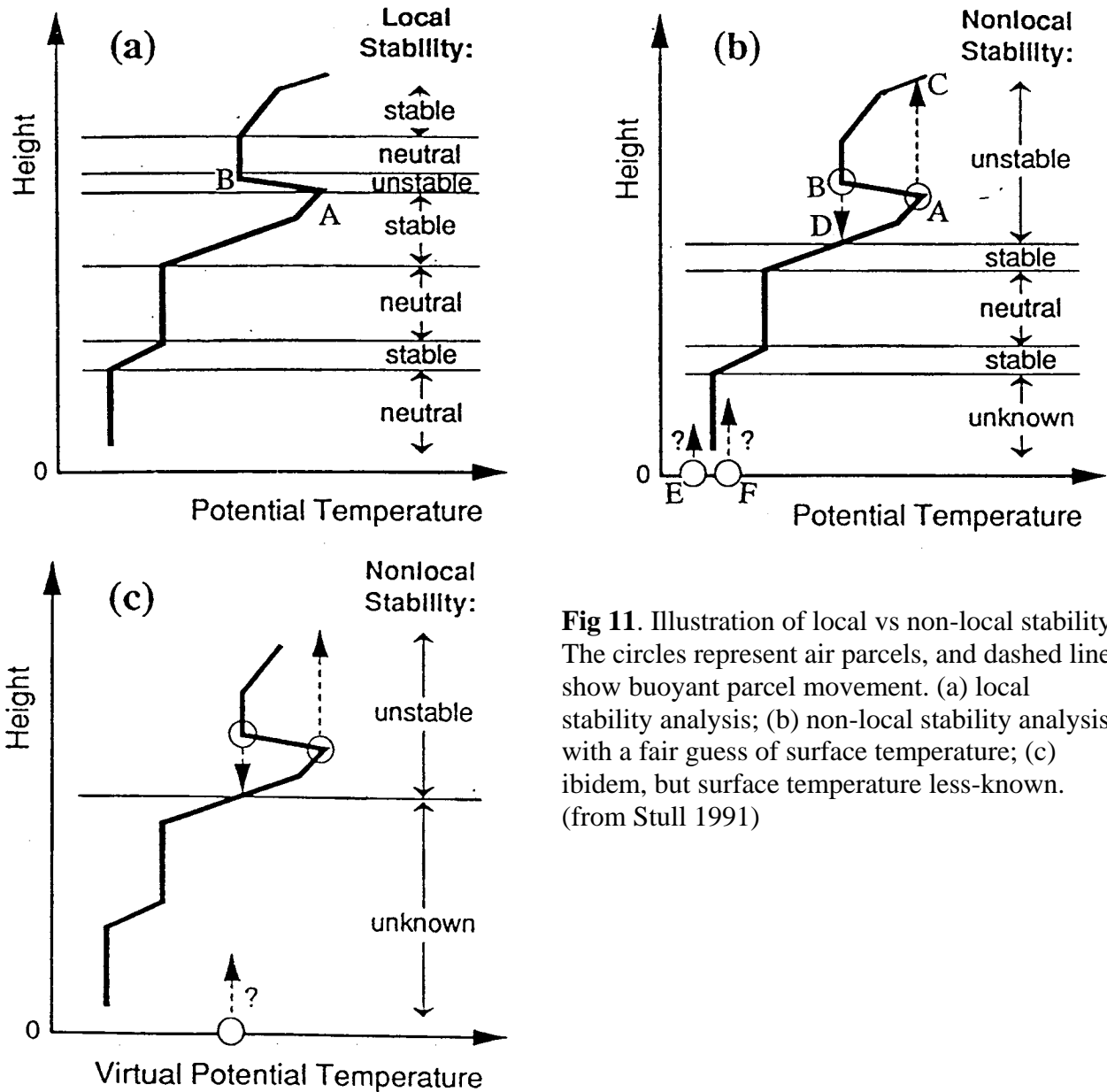


Fig 11. Illustration of local vs non-local stability. The circles represent air parcels, and dashed lines show buoyant parcel movement. (a) local stability analysis; (b) non-local stability analysis, with a fair guess of surface temperature; (c) ibidem, but surface temperature less-known. (from Stull 1991)

The non-local stability distribution is quite different (Fig 11b). The locally unstable layer (Fig 11a) is non-locally a much thicker layer, mainly because the amount of local instability is so large (compare to a ball on a steep hill). The non-locally unstable zone extends from the warm peak (A) upwards to where it intersects with the ELR (C), and from the coldest part of the locally unstable zone (B) downwards, again to the intersection with the ELR (at D). The latter can be understood by pushing a parcel downwards from B; it will be colder than the environment and continue downwards (unstable) until it reaches D. Beyond D, it would be warmer than the environment, and it would ascend, so it stalls at D. Only the locally stable zone below D is non-locally stable. In terms of non-local stability, the neutral and stable areas are smaller (Fig 11 b), and they may disappear in the vicinity of a strong locally unstable layer. Because in this case the ELR is unbounded, the non-local stability is theoretically entirely unknown. Practically, the potential temperature at the surface is estimated in Fig 11b between E and F, so only the non-local stability of the lowest layer is unknown. If the potential temperature at the surface was less certain, the non-local stability of a larger section would be unknown (Fig 11c). In what follows, we will focus on local and non-local stability in a confined domain with known boundaries.

(c) Absolute and conditional stability

Consider the diagram in Fig 12 to be a very much simplified version of an aerological diagram. The lapse rates in cases I,II and III are confined at the top and the bottom, in order to focus on local stability and ignore non-local effects. It can be seen that three possible cases (I,II, and III) of an actual ELR have been plotted onto the diagram: the SALR and DALR through a representative point P on the temperature profile have also been included.

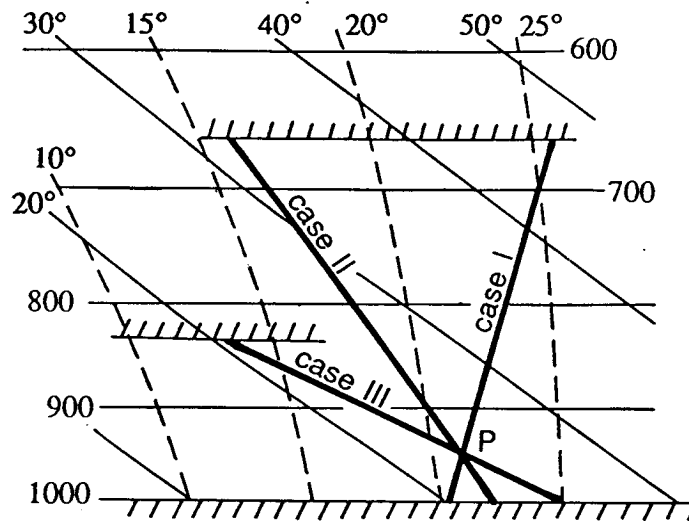


Fig 12. Case I is absolutely stable, case II conditionally stable, and case III absolutely unstable.

Case I: absolute stability: - In **Fig 13**, if the parcel was initially saturated, so that it would follow the moist adiabat when moved upward, it would still be colder than its surroundings (or warmer if moved downward) and thus would also be restored to its initial position. Again we have stability. The situation (or atmosphere) wherein either a dry or a saturated parcel is in a stable state is called an absolutely stable condition (or atmosphere).

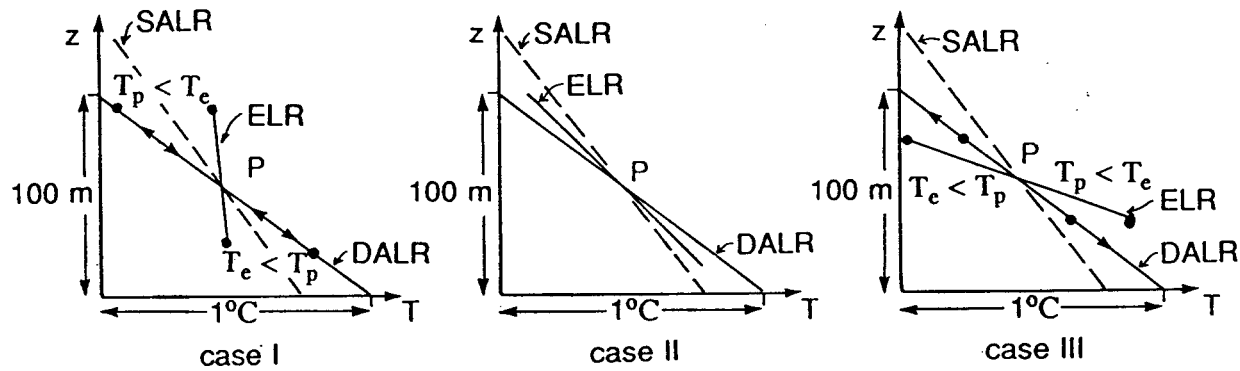


Fig 13. Three cases of stability (Fig 12) shown on a T-z diagram. The reference point is marked as P. After displacement, the parcel and ambient temperatures are denoted as T_p and T_e , respectively.

Case II: conditional instability: - using the arguments above it can be seen that if the parcel is dry, the atmosphere in case II will be stable. On the other hand, if the parcel was saturated, then lifting (moving it along the moist-adiabat) would make it warmer than the environment. It is therefore less dense and lighter, and must experience an upward force. It will move away from the point P for as long as it remains warmer than the air around it. Such a condition is unstable. In other words, instability of a layer is that state wherein, if a parcel is displaced even slightly from its original position, it will continue to move away. The arguments above will also show that a saturated parcel will continue to sink downward if depressed from point P, as long as moisture is available for evaporation upon warming. Since the stability depends on whether or not the parcel is dry, this situation is referred to as conditionally unstable. That is, the layer is stable when dry, unstable when saturated.

• *Case III: absolute instability:* - in this case, an analysis based on the procedures above will show that regardless of whether the parcel is dry or moist, it will always move away from P if it is displaced slightly, as shown in Fig 13. The environment is said to be in an absolutely unstable state.

This discussion is based on the diagram of the three possible general positions of the actual ELR and their relation to the DALR/SALR. The technique discussed above should enable you to determine the stability for any ELR, if you know the degree of saturation of the parcel. The latter can be determined by means of the DLR. Obviously, when $T = T_d$, then the parcel is saturated. Else, you know that a rising parcel becomes saturated when r_s is reached. The mixing ratio r is conservative for uplift, so the parcel is saturated when the mixing ratio at the dewpoint T_d is reached. Therefore, a parcel will ascent dry-adiabatically until it intersects with the saturation mixing ratio line through T_d at the reference level. From there on, it behaves like a saturated parcel.

The term neutral stability is used for all marginal cases: for instance, if the ELR coincides more or less with the DALR, the ELR is (dry) neutral. If the air is saturated and the ELR is very close to the SALR, then the ELR is moist neutral.

(iii) The slope technique

Now that you familiarized yourself with the parcel technique to analyze stability, you may know that there is another technique which is much quicker but not as intuitive. Referring to Fig 12, it can be seen that if the ELR, when plotted on the aerological diagram, is inclined to the left of DALR, it

corresponds to unstable conditions. By the same token, the conditionally unstable ELR has a slope which lies between the DALR and the SALR. And an ELR which is tilted to the right of SALR is stable. An isothermal ELR, for instance, is quite stable. An inversion is even more stable.

The lapse rate is merely change in temperature change in height and is positive when temperature decreases upward. Thus the lapse rate of profile I is less than the lapse-rate of II, which in turn is less than that of III. Following the argument it can be seen that:

- lapse rate I is less than both the dry and moist adiabatic lapse rates,
- lapse rate II is between the dry and moist adiabatic lapse rates,
- lapse rate III is greater than both the dry and moist adiabatic lapse rates.

Formalized verbally: there is

- absolute stability when the ELR is less than the SALR ($\gamma < \Gamma_s$);
- conditional instability when the ELR is greater than the SALR, less than the DALR ($\Gamma_s < \gamma < \Gamma_d$);
- absolute instability when the ELR is greater than the DALR ($\gamma > \Gamma_d$).

The DALR is symbolized by Γ_d , the SALR by Γ_s (see section 2.4), and the ELR by γ .

(iv) *Conditional instability*

Conditional instability can easily be determined from the slope of the ELR, as discussed previously. In the absence of an aerological diagram (e.g. in a NWP model), conditional instability can be determined via a simple criterion:

$$\boxed{\frac{d\bar{\theta}_e^*}{dz} < 0} \quad (36)$$

This criterion is similar to the criterion for absolute instability (35), but it involves the saturated equivalent potential temperature θ_e^* . This is not surprising, since both conditional instability and θ_e^* ignore the actual availability of water vapor. To prove (36), we follow an argument similar to the one that led to (35) (section 3.2). But now $\delta\theta$, the difference in potential temperatures between the parcel and the environment ($\theta_{\text{parcel}} - \theta_{\text{environment}}$), after lifting over a displacement δz , is

$$\delta\theta = (\bar{\theta} + \delta\theta_{\text{cond}}) - \left(\bar{\theta} + \frac{d\bar{\theta}}{dz} \delta z\right) = \delta\theta_{\text{cond}} - \frac{d\bar{\theta}}{dz} \delta z \quad (37)$$

where $\delta\theta_{\text{cond}}$ represents the condensational heating of the parcel (if it were saturated). From (21) it follows that $\delta\theta_{\text{cond}}$ can be approximated as,

$$\delta\theta_{\text{cond}} = -\bar{\theta} \frac{d}{dz} \left(\frac{Lq_s}{c_p T_v} \right) \delta z$$

Therefore the buoyancy of the parcel of air, $g \frac{\delta\theta}{\theta}$ (section 3.2), is, with (37):

$$g \frac{\delta\theta}{\theta} = -g \left\{ \frac{1}{\bar{\theta}} \frac{d\bar{\theta}}{dz} + \frac{d}{dz} \left(\frac{Lq_s}{c_p T_v} \right) \right\} \delta z = -g \frac{d}{dz} \left(\ln \bar{\theta} + \frac{Lq_s}{c_p T_v} \right) \delta z = -g \frac{d \ln \bar{\theta}_e^*}{dz} \delta z \quad (38)$$

following the definition of θ_e^* (24). Clearly, from (38) a modified Brunt-Vaisalla frequency can be derived, following the steps in (33). This *saturated Brunt-Vaisalla frequency* N_s is:

$$N_s^2 = g \frac{d \ln \theta_e^*}{dz} \quad (39)$$

(39) shows that a (necessary and sufficient) condition for conditional instability ($N_s^2 < 0$) is that the ambient θ_e^* decreases with height, i.e. criterion (36). This criterion should be compared to the one for absolute instability (section 3.2) and for potential instability (Section 3.5). The saturated Brunt-Vaisalla frequency N_s is the frequency of a (conditionally) stable parcel that is kept moist during the oscillation. Under the same environmental conditions, $N > N_s$ or the period for a dry parcel is shorter than the period for a moist parcel, in a stable environment. This is a factor in the explanation of the asymmetry of mountain lee waves and of downslope wind storms in the lee of mountains: the descent (dry) is faster than the ascent (moist).

Typical profiles of θ , θ_e , and θ_e^* in the vicinity of tropical deep convection are shown in **Fig 14**. Clearly, the lower troposphere is absolutely stable at all levels, but least so in the PBL. The lower half of the atmosphere (1000- 500 hPa) is conditionally unstable. However, this does not imply that convection spontaneously develops. The release of conditional instability requires saturation at some level. The lowest third of the atmosphere (1000-666 hPa) is potentially unstable, as will be discussed in Section 3.5.

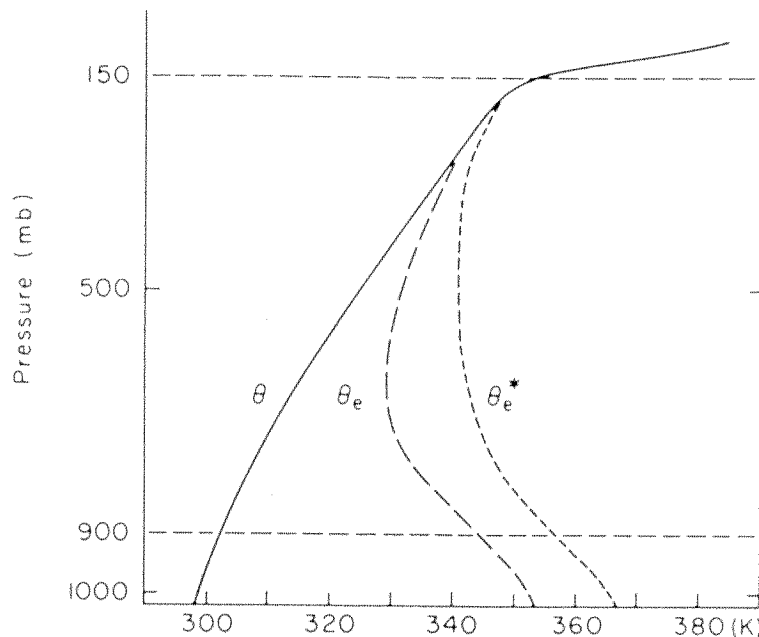


Fig 14. Typical sounding of θ , θ_e , and θ_e^* in the intertropical convergence zone. (from Holton '92).

Conditional instability is by no means uncommon. The reason why the instability rarely materializes into convection is that typically the atmosphere is fairly dry, even in the PBL. It is not easy to determine, in a conditionally unstable situation, how likely it is that unstable motions (convection) will develop. This depends on the details of the ELR and the DLR.

(v) *Convective available potential energy (CAPE), and convective inhibition (CIN)*

The only way to assess the likelihood of convection is by means of the parcel method. In **Fig 15** the parcel will certainly be buoyant for a considerable height; for example, at the level of maximum buoyancy, the parcel temperature T is larger the ELR temperature T_e . However, unless the parcel is saturated, it will follow at least a short section of dry adiabat before it ascends moist adiabatically. Notice that at the LCL, the parcel is colder than the environment (point D is colder than B, i.e. $T_D < T_B$). Therefore, even in the least stable situation of conditional instability, the parcel will be negatively buoyant when it penetrates through the first layers of air. So the parcel will need external energy to rise. The negative buoyancy is often referred to as *convective inhibition* CIN (Fig 15). The amount of energy required to penetrate to the *level of free convection* (LFC, Fig 15) is proportional to the area described by the ELR (line ABC) and the parcel trajectory (line ADC).

The source of this energy can be of two types:

- **sustained uplift:** - all the energy (CIN) is derived from the airflow. For instance: sustained lifting over a mountain or a frontal surface, the large scale lifting by upper level divergence due to changes in wind speed/direction aloft, or a frontogenetic circulation. Rapid updrafts occur within the convective PBL, in thermals, but these thermals are short-lived, and by themselves they will not penetrate the lid. The importance of sustained uplift is NOT to force the air through the CIN region (area ABCDA), but rather, to alter the T and T_d lines (see potential instability, thereby reducing the CIN, eventually allowing a lucky thermal to break through. The sustained mesoscale uplift itself is not the result of buoyancy, but rather is due to forced convergence (e.g. over a mountain) or to some dynamical response to a larger-scale imbalance.

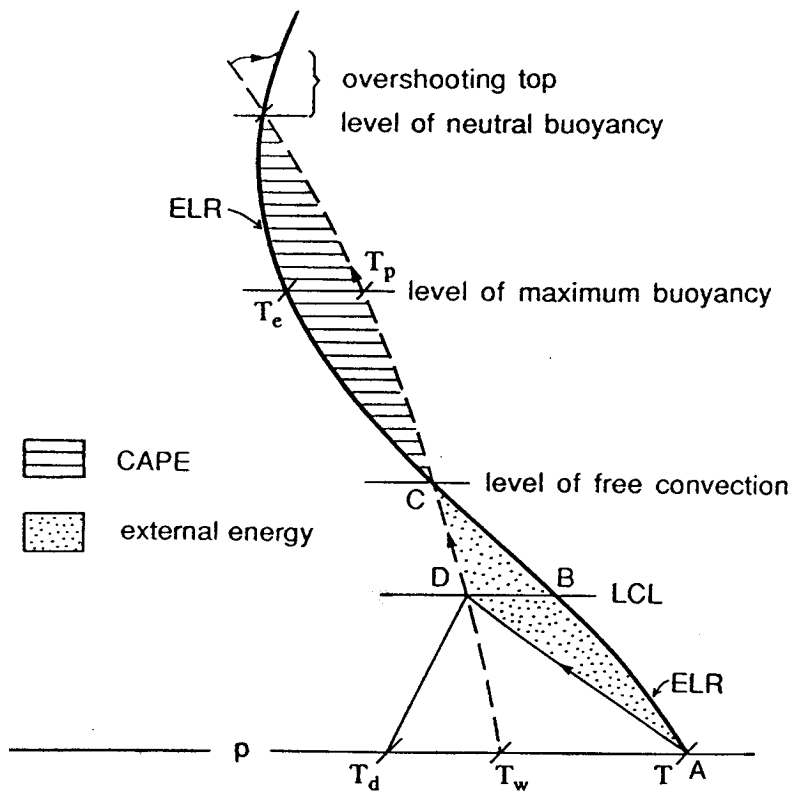


Fig 15. Parcel trajectory (thin line) vs the ELR (bold line). The parcel is shown as a solid line along a dry adiabat and a dashed line along a moist adiabat. The “external” energy is commonly known as CIN (convective inhibition).

• **thermal forcing:** - the size of the area ABCDA can be reduced by altering the temperature and/or dewpoint at the lower boundary. Thermal forcing also increases the area of positive buoyancy above the level of free convection. In other words, thermal forcing increases the moist static energy of the lower ELR, and increases the amount of energy that can be released by convection. Changes in moist static energy can be due to:

- direct (sensible) heating (**Fig 16a**), which occurs during the daytime over land; this effect raises the LCL (LCL₂ is higher than LCL₁)
- latent heating, i.e. the moistening of the lower layer (**Fig 16b**), which typically occurs by advection; this effect lowers the LCL.

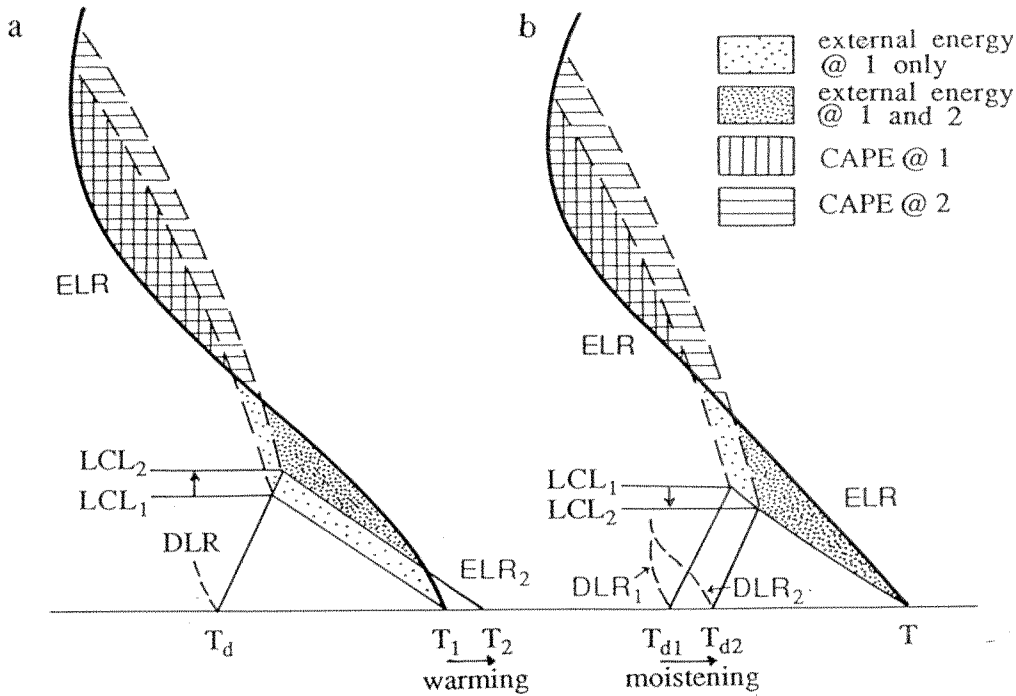


Fig 16. The effect of the increase of (a) temperature and (b) dewpoint on the LCL and the amount of CAPE and CIN.

The occurrence of anomalously hot and moist air is usually a reliable precursor of severe storms. However thermal forcing itself is often not sufficient. It usually only reduces the amount of sustained uplift required. It is rarely clear what exactly triggers the release of the instability. Notice also that the analysis presented here assumes that any thunderstorms resulting from conditional instability are relatively small; thunderstorm complexes (*mesoscale convective systems*) may impact directly on what is referred to as the ‘environmental’ lapse rate.

The ceiling of the convection is given as a first approximation by the *level of neutral buoyancy* LNB (Fig 15b). Thunderstorms occur in conditionally unstable situations. The vigor of a thunderstorm is proportional to the amount of potential energy it releases. Per unit mass, a parcel of depth dz has an amount of potential energy dP equal to its (upward) buoyancy force times vertical displacement dz:

$$dP = \frac{\delta\theta}{\theta} g dz \quad (40)$$

or, with the aid of (1) and (14), and assuming that $dp=0$ (see footnote 5),

$$dP = -R\delta T_v d \ln p \quad (41)$$

where δT_v is the virtual temperature difference between the parcel and the ELR.

dP , integrated from the level of free convection to the level of neutral buoyancy, is referred to as the convective available potential energy (CAPE) P ,

$$P = -R \int_{LFC}^{LNB} \delta T_v d \ln p \quad (P \geq 0)^{14} \quad (42)$$

which can visually be estimated by the shaded area in Fig 15, on a skew T. The integral (42) can be expressed in terms of finite differences, with a pressure increment of 10 hPa for instance. The CAPE equals the maximum amount of (potential) energy that can be released by a convective cloud (of unit mass). The larger the area (i.e., the larger the CAPE) and the smaller the area of CIN (external energy), the more likely the occurrence of a severe storm is. Therefore, the area of CAPE is often referred to as the positive area, whereas the area of CIN is called the negative area. CIN is calculated in the same way as (42), but the integral bounds are surface (or mixed-layer top) to LFC. Part of the CAPE, once released, is converted into the kinetic energy of the updrafts. In turn, this energy is lost by entrainment and by the penetration of an overshooting top into the stable environment above the LNB (Fig 15).

• Estimating CAPE (or CIN) from sounding data (without calculating parcel temperature).

According to parcel theory, the parcel temperature equals the surface wet-bulb potential temperature $\theta_{w,sfc}$ at all levels above the LCL, in other words, the parcel follows a moist adiabat from the LCL up. At any level i , the moist adiabat through the ambient air temperature T_i can be expressed as $\theta_{w,i}^*$, the saturated wet-bulb potential temperature. Note that θ_w^* relates to θ_w in the same way as θ_e^* relates to θ_e , i.e., it is assumed that the air is saturated. Then at any level i between the LFC and the LNB, $\delta T_i = \theta_{w,sfc} - \theta_{w,i}^*$, and thus CAPE can be estimated from sounding data as follows:

$$P = R \sum_i (\theta_{w,sfc} - \theta_{w,i}^*) \frac{\Delta p_i}{p_i} \quad \text{for all levels (i) where } \theta_{w,sfc} > \theta_{w,i}^* \quad (43)$$

The term $\frac{\Delta p_i}{p_i} = 2 \frac{p_i - p_{i+1}}{p_i + p_{i+1}}$ in finite differences. The advantage of this approach is that one can

readily redefine the parcel's moist adiabat. Sometimes the lowest 50-100 hPa are mixed first (constant θ and q). In terms of (43), the 'mixed-layer' CAPE is obtained by replacing $\theta_{w,sfc}$ by the

average wet-bulb potential temperature $\frac{1}{N} \sum_{ML} \theta_w$ over the mixed-layer (ML) depth.

¹⁴ Note that $P > 0$ since, in pressure units, $LFC > LNB$.

(vi) Latent instability

The ELR shown on Fig 17a is of little concern, whereas a thunderstorm is likely with the ELR on Fig 17b. Notice that not all conditionally unstable soundings display an area of positive buoyancy. A conditionally unstable sounding with, at some level, an area of positive buoyancy (e.g. Fig 17 a-b) is said to have *latent instability*, which is a non-local condition. Conditional instability is a necessary condition for latent instability; the reverse cannot be said, as shown in Fig 17c.

Also notice that point A in Fig 15 does not necessarily correspond with the ground level. Convection normally starts from the level that demands the least amount of external energy. “Elevated convection” is rare in Laramie but quite common in the southeastern US in the spring and fall seasons. In order to evaluate the occurrence and intensity of latent instability in a conditionally unstable sounding, it is useful to construct the *wet-bulb temperature lapse rate* (WLR) from a combination of the ELR and the DLR using Normand’s proposition, as shown in Fig 18.

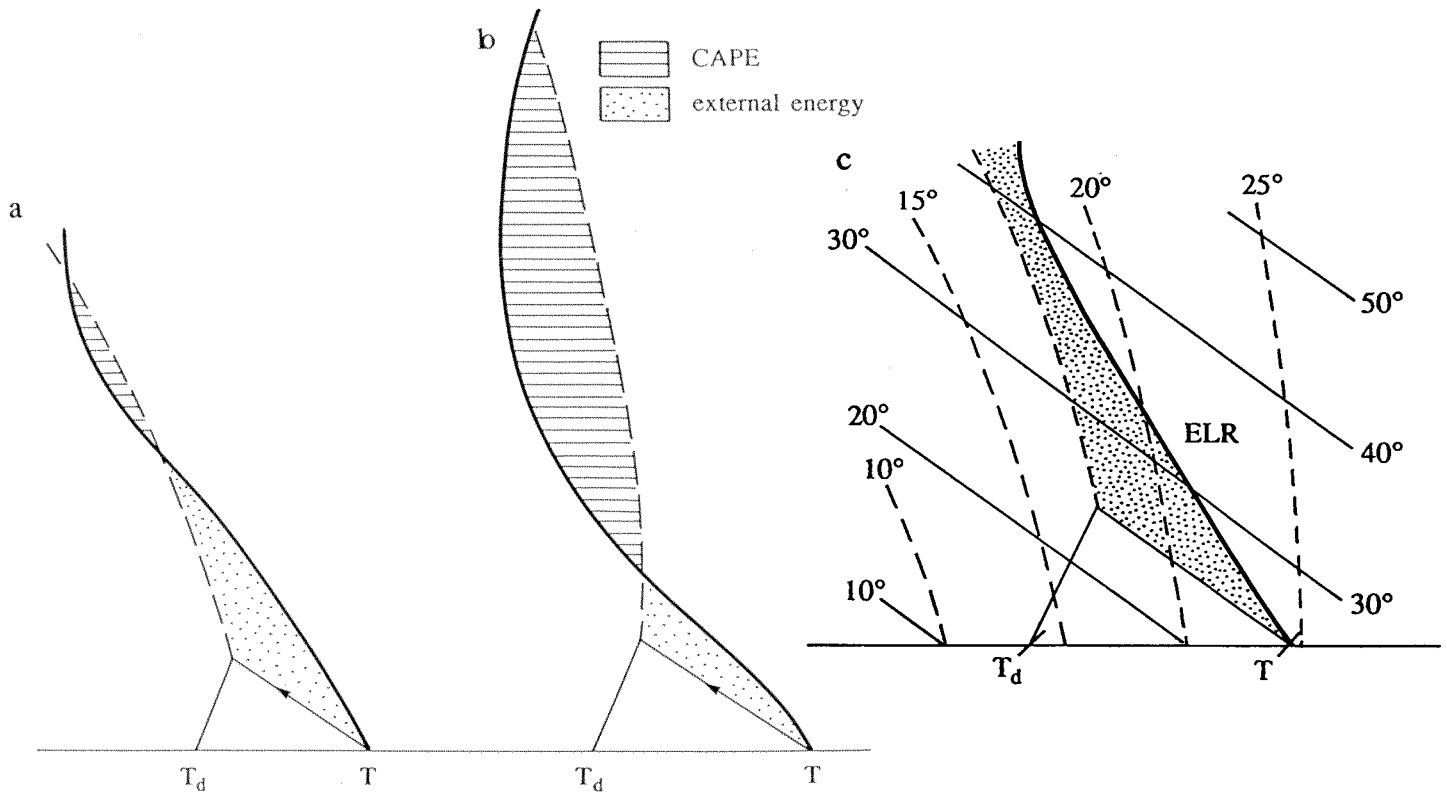


Fig 17.(a-b) soundings with CAPE (i.e. latent instability).(c) a sounding with conditional instability, but without latent instability.

The WLR is useful because all vertical displacements occur strictly along a SALR from any point on the WLR (this follows from the definition of the LCL and Normand’s proposition). One can then simply follow a moist adiabat from any point on the WLR, upward, and see whether this moist adiabat intersects with the ELR. If it does, then there is latent instability. In Fig 18, a parcel rising from the ground (line AX) would not intersect the ELR at any level. At 850 hPa however, there is latent instability: a parcel lifted from 850 hPa (line BCD) crosses the ELR and is warmer than the environment between 700 and 400 hPa. Analysis of a series of moist adiabats from the WLR shows

that the sounding has latent instability from level 960 to 750 hPa¹⁵. This instability is maximum at 850 hPa. Therefore at 850 hPa, any triggering will release the most intense convection. Forecasters will then examine whether there is any indication of possible triggering at that level, e.g. by frontal ascent. Notice that the height of maximum latent instability can change rapidly, and that on warm, sunny days it usually drops to the ground level.

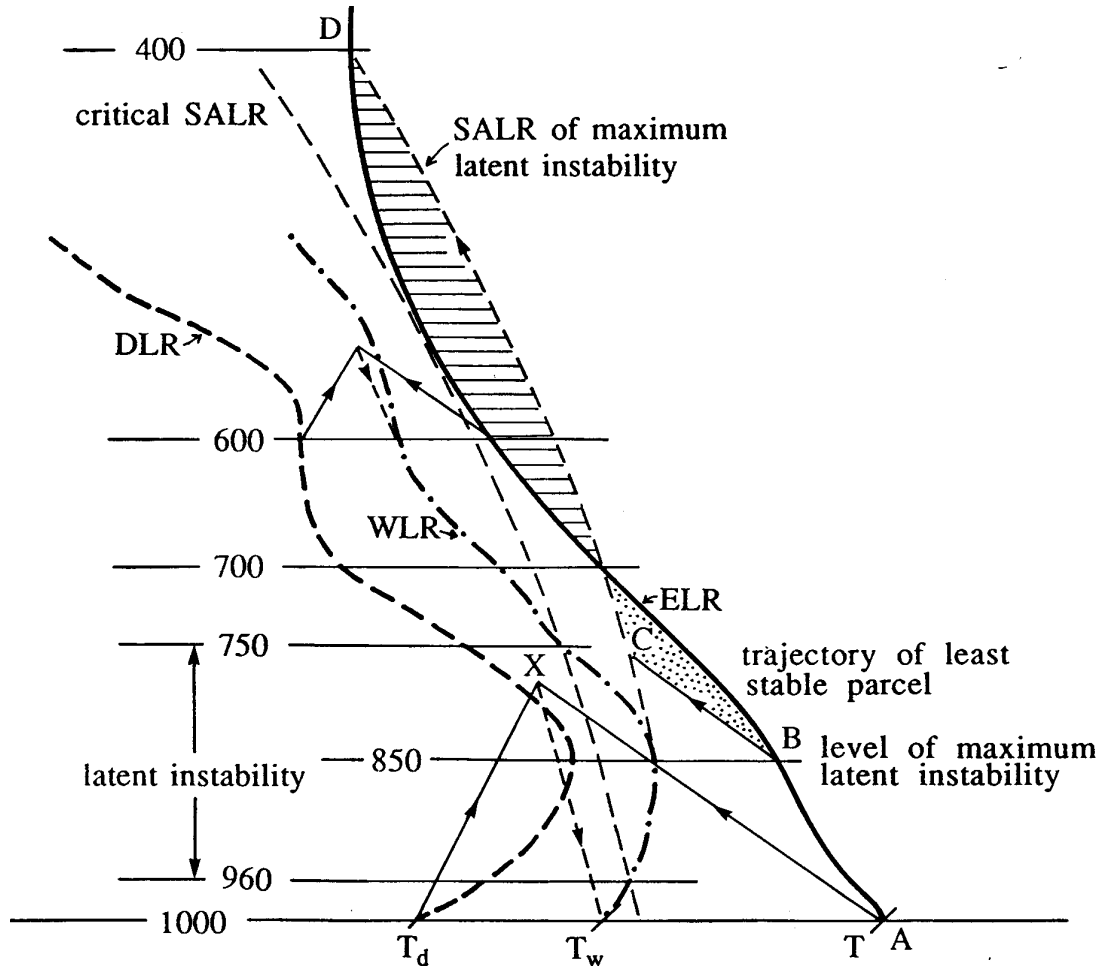


Fig 18. The evaluation of latent instability. Typically the ELR (solid line) and the DLR (dashed line) are based on observations, and the WLR (dash-dot line) is derived at each level, using Normand’s proposition. The procedure is shown explicitly at just two levels, 1000 and 600 hPa. The shaded areas show the CIN and CAPE associated with a parcel at the level of highest latent instability, i.e. 850 hPa in this case.

¹⁵ It is a common mistake to claim that the profile has latent instability where the parcel is warmer than the environment, e.g. between 700 and 400 hPa for a parcel starting at 850 hPa. Latent instability is assessed at the parcel’s source level, i.e. at 850 hPa.

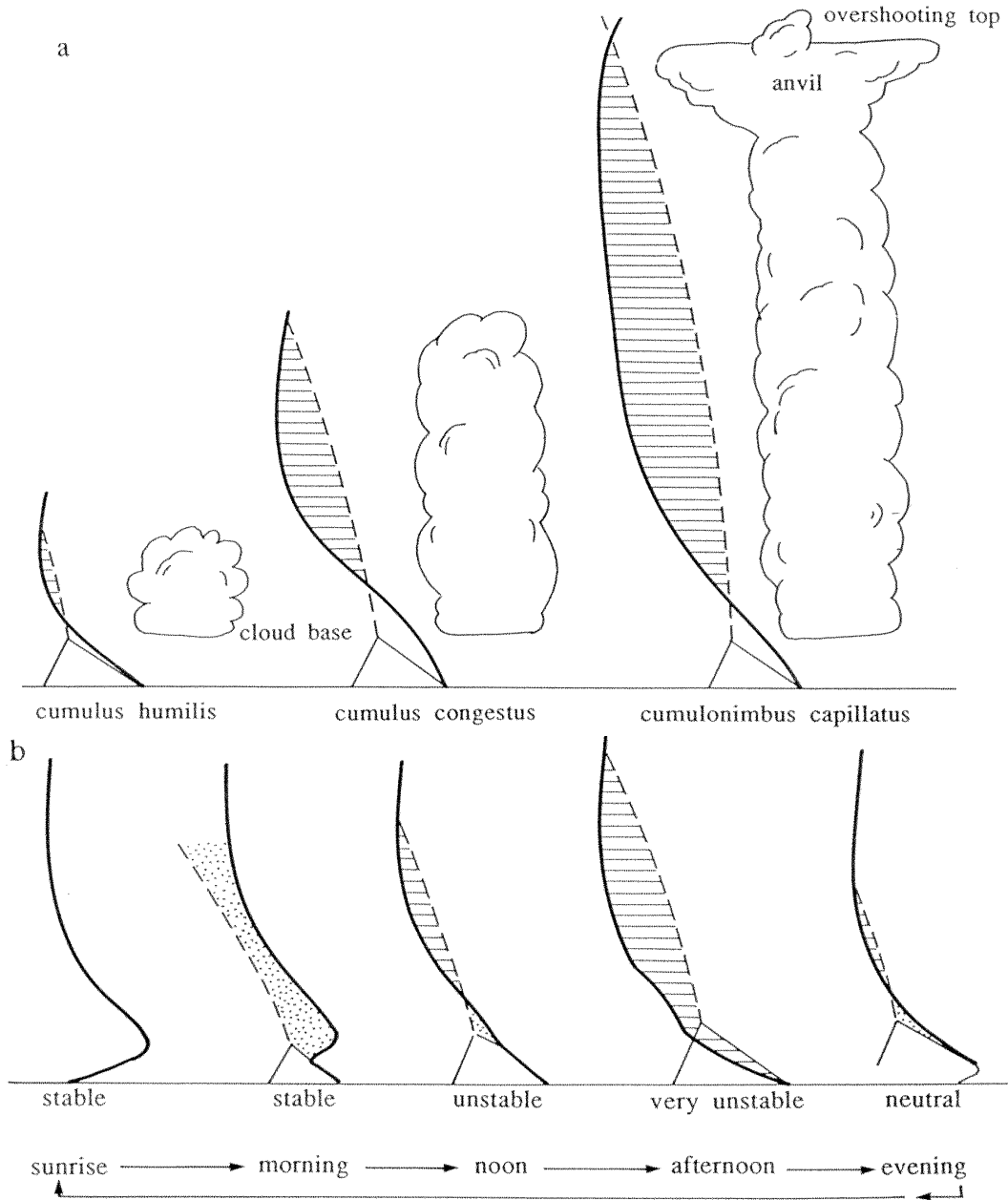


Fig 19. (a) The convective cloud population is trimodal in the tropics (Johnson et al 1999); each type corresponds to different ambient conditions (ELR/DLR). (b) Diurnal cycle of the convective boundary layer, building CAPE, and the more shallow nocturnal radiation inversion. This cycle is obvious in the high Rockies in summer, leading to thunderstorms almost every afternoon.

The amount of CAPE is a function of both the buoyancy of the parcel (or the instability of the ELR) and the vertical depth of the positively buoyant area. Various types of cumulus and cumulonimbus clouds are associated with an increasing vertical depth of the positively buoyant area (**Fig 19**). Providing no change in airmass occurs (i.e. the moisture content remains the same), then morning and early afternoon heating and evening cooling of the PBL will produce a diurnal cycle in the occurrence and depth of convection, with a peak in convective activity in the afternoon (**Fig 19b**) This cycle is remarkably common over the Rocky-Mountain high terrain in summer. Elsewhere,

convective and larger scale dynamics usually alter the phase and the amplitude such a cycle. In any event, CAPE is an important variable for the understanding and forecasting of convection.

(vii) *Potential instability*

So far we have analyzed the stability of a sounding by rising or lowering an air parcel from a certain level and by comparing its temperature with the environment. Now we will examine the effect the lifting of an entire layer has on the stability of that layer. This issue is important because most lifting mechanisms act on a scale much larger than a convective cloud.

In **Fig 20a**, an absolutely stable layer AB is shown between 900 and 800 hPa. This layer is 100 hPa thick, which corresponds to about 1 ton of air per square meter (that follows from the hydrostatic equation). If the air does not diverge in this layer, and typically the divergence is very small, then the layer will still have the same mass when lifted over some distance. Therefore, the layer will still be 100 hPa deep when the bottom is lifted to 700 hPa. We assume that the air is dry enough that no condensation occurs in the lifting. Notice that the layer is now conditionally unstable (Fig 20a, line CD). Clearly, lifting is destabilizing.

Clear destabilization occurs when lifting a layer of air whose lower part is relatively more moist. In Fig 20b, a WLR is derived again from the DLR and the ELR (Normand's principle). You should reiterate at this point that on an aerological diagram at any level a parcel, lifted from the ELR, ascends along a DALR until it intersects with the moist adiabat through the wet-bulb temperature at that level (see Fig 18). Again, we start from an absolutely stable layer AB that is lifted over a depth of 200 hPa. In this case, the lower part of the layer reaches saturation quickly (A to C), whereas the top part ascends dry adiabatically up to just below the 600 hPa level (B to D). At this point, the profile of the layer CD is conditionally unstable, and since it is saturated, the instability is immediate. This is referred to as *potential instability* of the layer AB. The entire layer will now rise along a moist adiabat.

Potential instability is the dominant mechanism of thunderstorm outbreaks, e.g. along a cold front, over a warm front, or near a dryline. It is believed to be important also in the case of the widespread fairly heavy rain embedded within lighter rain in extratropical disturbances. Theoretically, the rising will continue until the layer intersects with the ELR. It is not obvious where the ELR is, because the lifting of an entire layer also displaces the layers above. These layers are not necessarily potentially unstable, and therefore, they may resist any further lifting. Therefore, rather than a smooth lifting of the entire potentially unstable layer, one may rather observe small turrets or bands penetrating through the more stable layers aloft. This theory has been used for instance to explain the existence of multiple rainbands (5 to 50 km wide) within a front. In any event, even in the least stable case, the penetration depth of a convectively unstable layer will always be constrained by the tropopause.

The analysis of a set of soundings will show that a simple criterion exists for potential instability: *a layer is potentially unstable when the WLR tilts to the left of the moist adiabats*. Notice that this criterion concerns the slope of the WLR, and not the ELR, as for conditional instability. The criterion is the same as saying that the *wet-bulb potential temperature θ_w decreases with increasing height*. To convince yourself, determine θ_w at various levels on Fig 18. Clearly, θ_w is simply the value of the moist adiabat at any point along the WLR. Now to say that θ_w decreases with height is to say that the moist (potential) energy decreases with height, hence the name potential instability.

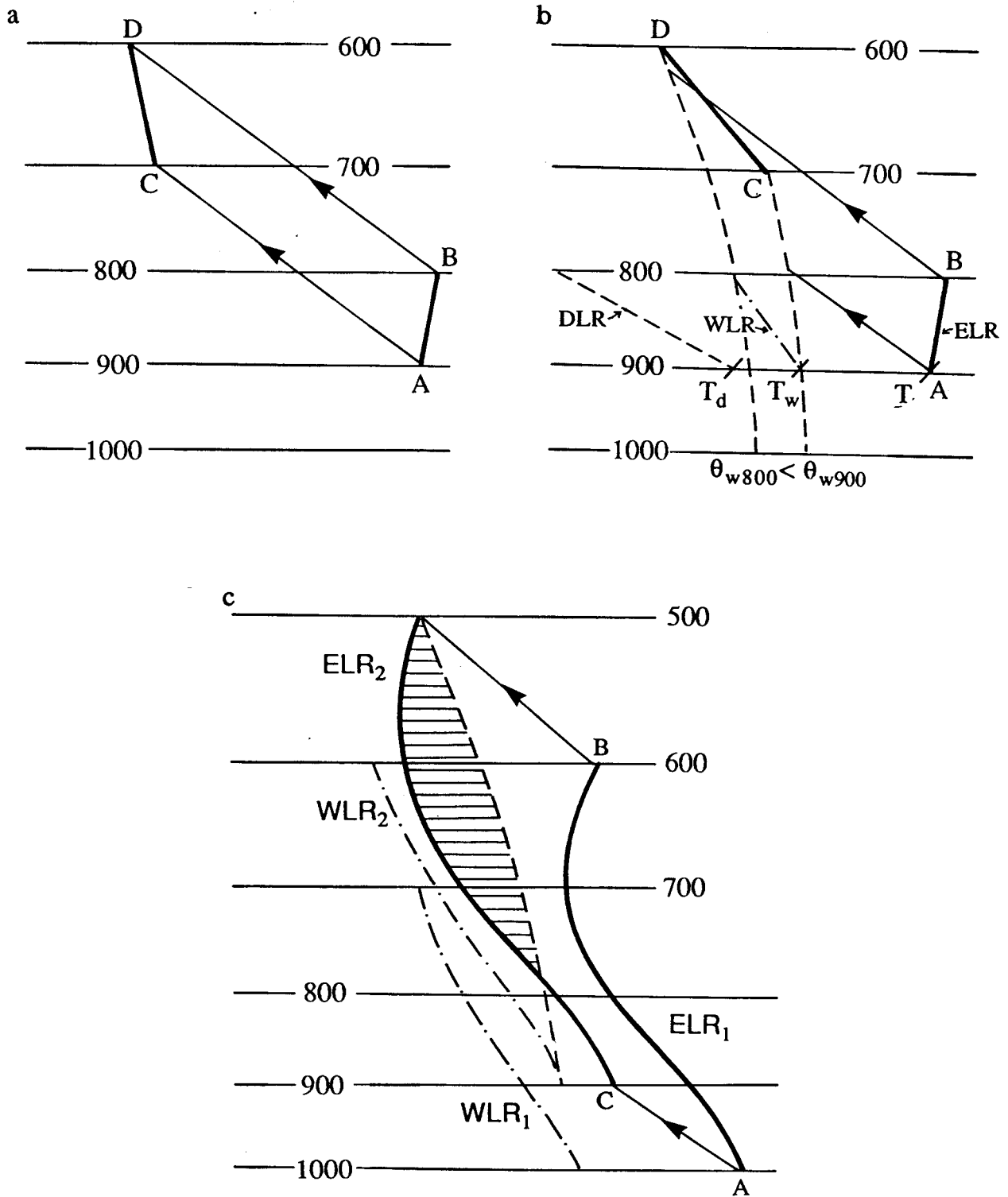


Fig 20. (a) Destabilization of a layer of dry air (A-B) by lifting, in this case over 200 hPa; (b) a potentially unstable layer is lifted enough to continue to rise; (c) development of latent instability by large-scale, deep lifting.

Mathematically, the argument is as follows: potential instability occurs when a layer of air, after being lifted to the point where it is saturated, finds itself unstable. That only occurs when that lifted layer of air is conditionally unstable, i.e.

$$\frac{d\bar{\theta}_e^*}{dz} < 0 \quad (36)$$

but the layer of air up there is saturated, so $\theta_e = \theta_e^*$, and also

$$\frac{d\bar{\theta}_e}{dz} < 0$$

Now θ_e is conserved in the case of both dry and saturated adiabatic vertical motion (θ_e^* is only conserved in saturated adiabatic processes). So we can return to the layer's source, where the layer was dry (not saturated), while conserving θ_e , so still:

$$\boxed{\frac{d\bar{\theta}_e}{dz} < 0} \quad (44)$$

This then is the criterion for potential (also called convective) instability (for a layer of air).

Note that $\frac{d\theta_e}{dz} = \frac{d\theta_w}{dz}$, since both θ_e and θ_w can be used to label moist adiabats (see Section 2.4).

Both conditional and potential instability require external lifting in order to realize the instability. *Conditional instability is conditional to the degree of saturation of the parcel*, and latent instability is conditional to the details of the ELR. *Potential instability occurs when the moist potential energy of a layer decreases with height.*

Fig 20a illustrated that the lifting of a layer may render the air conditionally unstable. Fig 20c shows that even latent instability can be realized by layer lifting. The sounding has some conditional instability at first (AB), but not any latent instability, because the air is too dry. Clearly, lifting of the entire column over 100 hPa (to CD) removes this restriction and makes the sounding rich in CAPE. Strictly speaking, the concept potential instability is used only when lifting renders the layer immediately unstable. But the difference is of little relevance. It is more important to realize that lifting generally destabilizes the environment. This explains in part the orographic enhancement of precipitation: not only does the air rise to cross the mountain crest. Often it rises much more, buoyantly so.

It is also important to realize that any moistening or warming of the lower layers in the troposphere, and any cooling of the upper troposphere, will make vertical instability more likely. Surface heating occurs diurnally; significant changes in stability can occur via differential advection. In the Great Plains, as well as in N. Argentina and Eastern Australia, severe thunderstorms occur typically when low level warm, moist air is advected poleward under an upper level wedge of relatively cold air moving in from the west. The destabilization is enhanced by the presence of sloping terrain (the Great Plains, the Mato Grosso, and the Great Dividing Range), which enhance large scale uplift. Destabilization is occasionally also enhanced by the equatorward penetration of a cold front, which acts like a mountain for the warmer poleward flow.

(viii) Profiles of θ , θ_e , and θ_e^* and CAPE

Typical profiles of θ , θ_e , and θ_e^* were shown in Fig 14. Clearly conditional instability typically occurs over a greater depth than potential instability. **Fig 21** shows the θ_e^* profiles for two tropical regions. From the θ_e^* profile and θ_e at the surface ($\theta_{e,sfc}$), one can obtain the LFC as the level where the $\theta_{e,sfc}$ value intersects the ambient θ_e^* curve. The reason why this intersection is the LFC is that the θ_e of an undiluted parcel rising from the surface is conserved, thus above the LFC, where the parcel is saturated, the parcel θ_e (or moist static energy) is larger than the ambient θ_e^* . On the aerological diagram, the difference between the parcel's moist adiabat (θ_e or θ_w) and the ambient temperature (in terms of moist adiabats on the diagram, this is the ambient θ_e^*) is a measure of the CAPE ($J\ kg^{-1}$), at least when integrated vertically from the LFC to the LNB. The latter is the level where $\theta_{e,sfc}$ rejoins the ambient θ_e^* curve (Fig 16). CAPE can then be calculated (see, e.g., Petersen and Rutledge 2001, Geerts and Dejene 2005) as:

$$CAPE = R \int_{LFC}^{LNB} (\theta_{e,sfc} - \theta_e^*) d \ln p \tag{45}$$

This expression (45) is a continuous (integral) version of (43). Clearly, on a θ_e -log p graph, CAPE is proportional to the area shaded in Fig 21. In the Sahel wet season the surface temperature is higher than in the Amazon, but it is drier, thus the LCL and LFC are higher, yet the CAPE is larger. The result is more intense, deeper storms than in the Amazon, but less rain. Amazon thunderstorms are closer to the maritime type, while Sahel thunderstorms are epitomically continental.

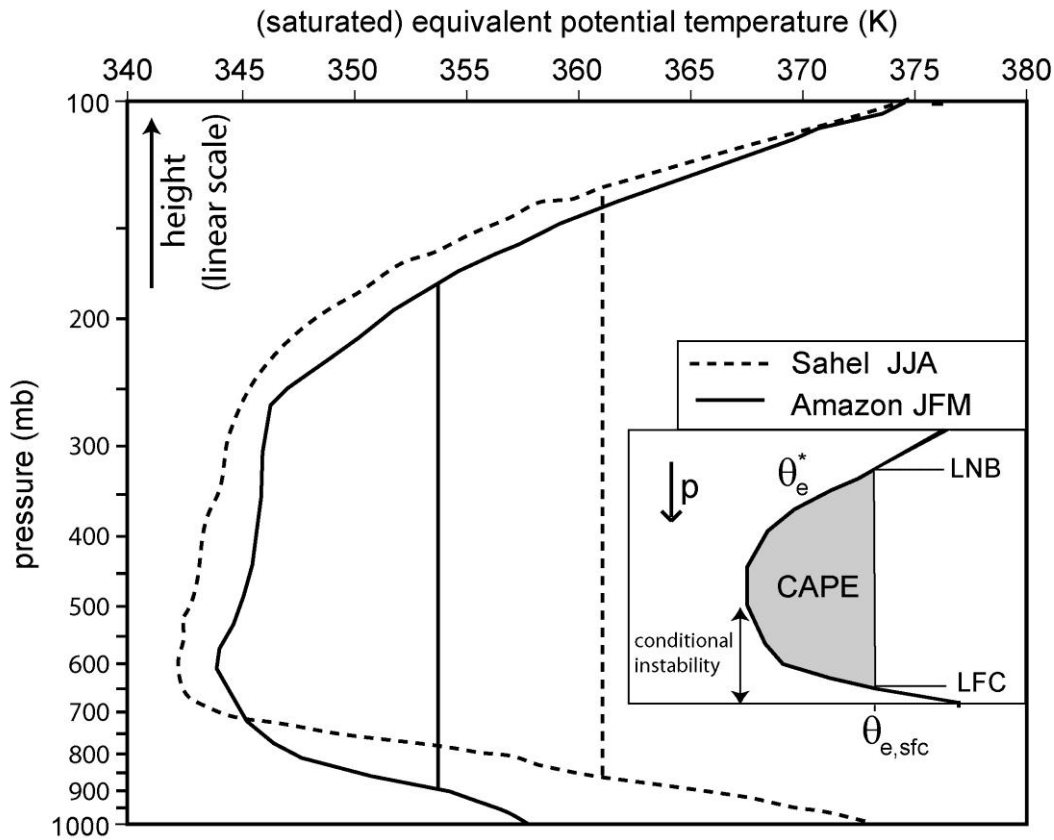


Fig 21. Climatological θ_e^* profiles for the Sahel (Africa) and the central Amazon during their corresponding wet seasons. The profiles are based on the NCAR/NCEP reanalysis dataset.

(ix) Stability indices

It would be useful to be able to express the degree of instability by a single index. This renders an examination of a large series of atmospheric soundings unnecessary, and allows the mapping. NWP model output or satellite sounder information allows plotting and contouring of that index, which makes a good forecasting tool. Several indices have been developed for this purpose. The names and exact formulae are only given for your further reference, in **Table 2**. They can be grouped in two types:

- **parcel temperature indices:** a parcel is lifted from a prescribed level to another prescribed level, at which its temperature is compared with the environment. The two most common indices used are the lifted index and the Showalter index (Table 2). By definition, the indices have to be negative for any possibility for thunderstorms. For the lifted index, the predicted afternoon maximum temperature at the surface can be used, rather than the observed surface temperature at the time of the sounding (especially if it is in the morning). Or the mean potential temperature and mixing ratio in the lowest 50-100 hPa can be used to determine the ‘best’ parcel trace. The value of these indices can be calculated on an aerological diagram, as illustrated in **Fig 22**. Table 2 also lists two modified indices, which involve more parameters. These modified indices may be more reliable, but they involve a calculation rather than simply a graphical estimation on the aerological diagram.

- **fixed-level temperature & dewpoint indices:** these are empirical formulae based on observations of T and T_d at various levels. The parcel technique is not used. The total totals index and the Whiting index are most commonly used. Exactly what values these indices assume when thunderstorm development can be expected is not clear, but a guideline for the critical values is given in Table 2.

index	definition	thunderstorms are possible if	severe thunderstorms are likely if
Lifted index	$LI = T_{500} - T_{pmax}$	$LI < 0$	$LI < -8$
Showalter index	$SI = T_{500} - T_{p850}$	$SI < 0$	$SI < -4$
Modified LI	$MLI = LI + (1000 - LCL)/15 + 8$	$MLI < 0$	$MLI < -8$
Modified SI	$MSI = SI + 0.7(T_{700} - T_{d700}) - 5$	$MSI < 0$	$MSI < -4$
Total totals index	$TT = T_{850} + T_{d850} - 2T_{500}$	$TT > 40$	$TT > 55$
Whiting index	$WI = T_{850} + T_{d850} + T_{d700} - T_{700} - T_{500}$	$WI > 15$	$WI > 35$

Table 2. Some stability indices. T_{pmax} is the surface daytime maximum temperature, cooled by lifting from the surface to 500 hPa, and T_{p850} is the temperature of a parcel lifted from 850 hPa to 500 hPa. At any pressure level (say 850 hPa), T_{d850} is the dewpoint and T the (dry bulb) temperature. LCL is the lifting condensation level (in hPa). All temperatures are expressed in °C or K.

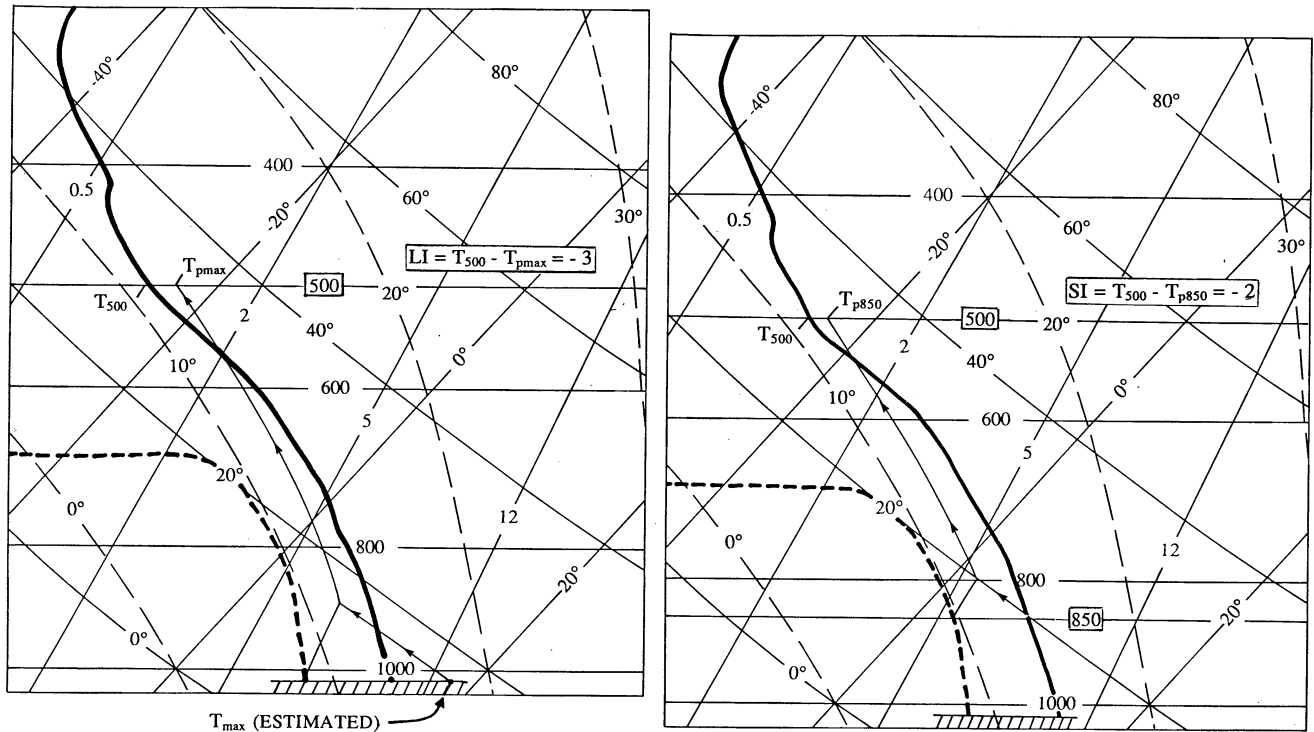


Fig 22. The calculation of the lifted index (LI), left, and the Showalter index (SI), right.

References

- Geerts, B. and T. Dejene, 2005: Regional and diurnal variability of the vertical structure of precipitation systems in Africa, based on spaceborne radar data. *J. Climate*, **18**, 893-916.
- Johnson, R. H., T. M. Rickenbach, S. A. Rutledge, P. E. Ciesielski, and W. H. Schubert, 1999: Trimodal characteristics of tropical convection. *J. Climate.*, **12**, 2397–2418.
- Manual of Meteorology, 1975: Australian Bureau of Meteorology, Rev. Ed. Pt. 1, General Meteorology, QC864-A8/1975.
- Petersen, W. A., and S. A. Rutledge, 2001: Regional variability in tropical convection: Observations from TRMM. *J. Climate*, **14**, 3566-3586.
- Preston-Whyte and Tyson, 1988: *The Atmosphere and Weather of Southern Africa*. Oxford University Press, 375 pp. QC991.A1.P74.
- Stull, R.B. 1991: Static Stability - an update. *Bull. Amer. Meteor. Soc.*, **72**, 1521-1529